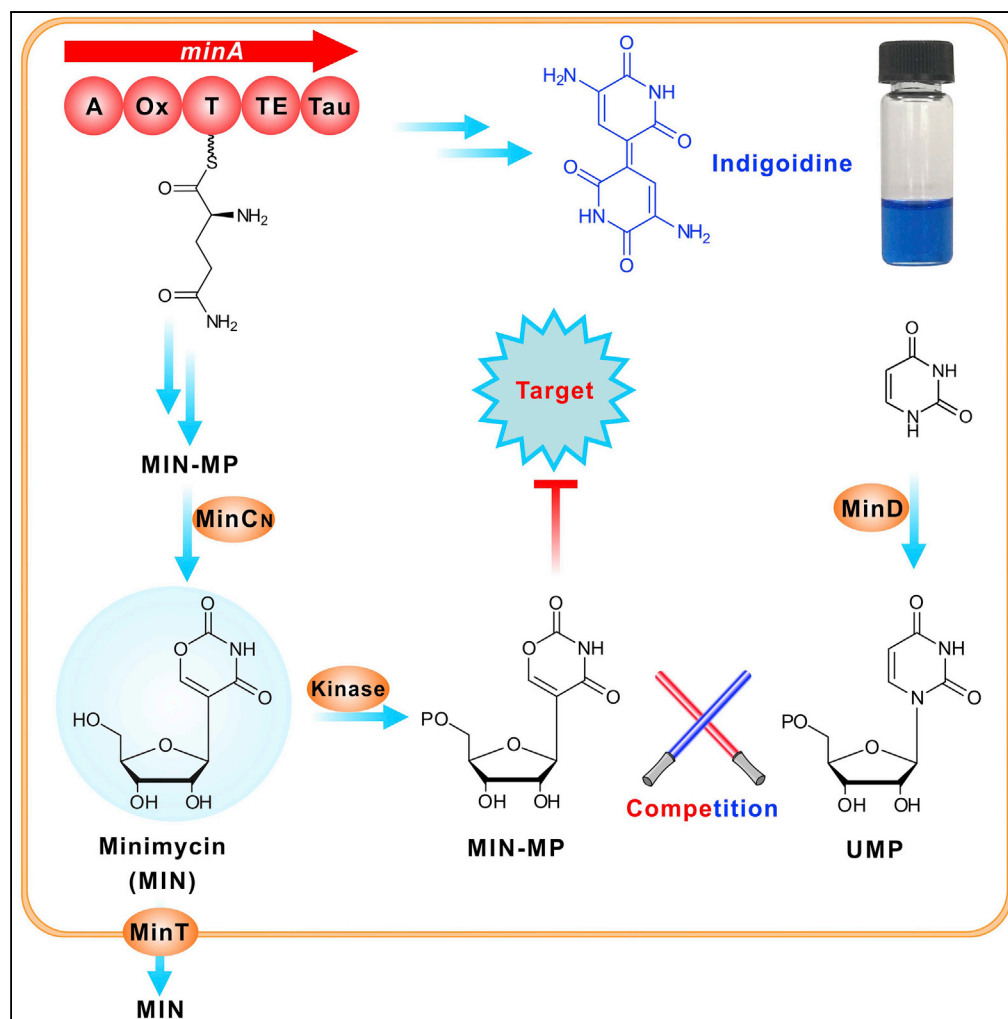


Article

Divergent Biosynthesis of C-Nucleoside Minimycin and Indigoidine in Bacteria



Liyuan Kong,
Gudan Xu, Xiaoqin
Liu, ..., Zixin Deng,
Neil P.J. Price,
Wenqing Chen

wqchen@whu.edu.cn

HIGHLIGHTS

A minimal 5-gene cluster (*min*) is essential for minimycin biosynthesis

Divergent biosynthesis of minimycin and indigoidine is mediated by an NRPS enzyme

A cascade of three safeguard enzymes constitutes the unusual self-resistance system

MinD functions as the key safeguard enzyme by increasing the UMP pool *in vivo*

Kong et al., iScience 22, 430–440
December 20, 2019 © 2019
The Author(s).
<https://doi.org/10.1016/j.isci.2019.11.037>

Article

Divergent Biosynthesis of C-Nucleoside Minimycin and Indigoidine in Bacteria

Liyuan Kong,^{1,4} Gudan Xu,^{1,4} Xiaoqin Liu,^{1,4} Jingwen Wang,¹ Zenglin Tang,¹ You-Sheng Cai,¹ Kun Shen,¹ Weixin Tao,¹ Yu Zheng,² Zixin Deng,¹ Neil P.J. Price,³ and Wenqing Chen^{1,5,*}

SUMMARY

Minimycin (MIN) is a C-nucleoside antibiotic structurally related to pseudouridine, and indigoidine is a naturally occurring blue pigment produced by diverse bacteria. Although MIN and indigoidine have been known for decades, the logic underlying the divergent biosynthesis of these interesting molecules has been obscure. Here, we report the identification of a minimal 5-gene cluster (*min*) essential for MIN biosynthesis. We demonstrated that a non-ribosomal peptide synthetase (MinA) governs “the switch” for the divergent biosynthesis of MIN and the cryptic indigoidine. We also demonstrated that MinC_N (the N-terminal phosphatase domain of MinC), MinD (uracil phosphoribosyltransferase), and MinT (transporter) function together as the safeguard enzymes, which collaboratively constitute an unusual self-resistance system. Finally, we provided evidence that MinD, utilizing an unprecedented substrate-competition strategy for self-resistance of the producer cell, maintains competition advantage over the active molecule MIN-5'-monophosphate by increasing the UMP pool *in vivo*. These findings greatly expand our knowledge regarding natural product biosynthesis.

INTRODUCTION

The C-nucleoside antibiotics (Figure 1) constitute an important sub-group of microbial natural products with unusual structural features and diverse biological activities (Isono, 1988; Maffioli et al., 2017). Their biosynthesis generally follows a succinct logic, with sequential modifications of simple precursors originating from primary metabolism (Hong et al., 2019; Isono, 1988; Palmu et al., 2017; Sosio et al., 2018; Wang et al., 2019). Less typically, minimycin (MIN, also called oxazinomycin) is produced by diverse bacterial strains, either *Streptomyces* sp. or *Pseudomonas* sp., and shows prominent antimicrobial activities against both Gram-positive and Gram-negative bacteria (Kusakabe et al., 1972; Tymiak et al., 1984). It has also demonstrated antitumor activity against transplantable tumors (Kusakabe et al., 1972).

MIN is structurally similar to pseudouridine, a modified nucleoside that is found abundantly in tRNA (Li et al., 2016). The MIN molecule has a unique structural feature in which a 1,3-oxazine 2,4-dione ring and a ribosyl sugar are linked via a C-glycoside bond (Sasaki et al., 1972) (Figure 1). Previous metabolic labeling studies have shown that the ribosyl portion of MIN derives directly from D-ribose (Isono and Suhadolnik, 1975, 1977), and C-6, C-5, and C-4 of the oxazine ring arise from the corresponding C-3, C-4, and C-5 of L-glutamate (Isono and Suhadolnik, 1977). Metabolic feeding experiments by Isono et al. showed that the C-2 of MIN is derived from carbon dioxide (Isono and Suhadolnik, 1975). Concomitant chemical synthesis of MIN was also achieved, with the finding that the synthetic form of MIN shares identical biological features with that from microbial source (De Bernardo and Weigele, 1977).

Indigoidine (Figure 1) is a bipyridyl pigment that was first documented as a microbial natural product in the 1960s (Kuhn et al., 1965), and later discovered to be produced by surprisingly diverse microbes (Heumann et al., 1968; Starr et al., 1966). The indigoidine biosynthetic gene cluster was initially reported from *Dickeya dadantii* (formerly known as *Erwinia chrysanthemi*), and it was revealed that it has important roles in pathogenicity and self-resistance to oxidative stress (Reverchon et al., 2002). The gene for indigoidine biosynthesis was later identified from diverse *Streptomyces* strains (Novakova et al., 2010; Pait et al., 2017; Yu et al., 2013). A single module non-ribosomal peptide synthetase (NRPS), which selectively recognizes L-glutamine as the starter substrate, was necessary for indigoidine biosynthesis (Brown et al., 2017; Takahashi et al., 2007). The indigoidine NRPS gene was subsequently engineered as a promising tool for synthetic biology purposes, either for natural product discovery (Olano et al., 2014) or as a reporter system (Muller et al., 2012; Rezuchova et al., 2018; Xie et al., 2017). More recently, Ankanahalli et al. have created a transgenic blue rose by introduction of a bacterial indigoidine biosynthesis gene

¹Key Laboratory of Combinatorial Biosynthesis and Drug Discovery, Ministry of Education, and School of Pharmaceutical Sciences, Wuhan University, Wuhan 430071, China

²State Key Laboratory of Food Nutrition and Safety, Tianjin Engineering Research Center of Microbial Metabolism and Fermentation Process Control, and College of Biotechnology, Tianjin University of Science & Technology, Tianjin 300457, China

³Agricultural Research Service, US Department of Agriculture, National Center for Agricultural Utilization Research, Peoria, IL, USA

⁴These authors contributed equally

⁵Lead Contact

*Correspondence: wqchen@whu.edu.cn

<https://doi.org/10.1016/j.isci.2019.11.037>



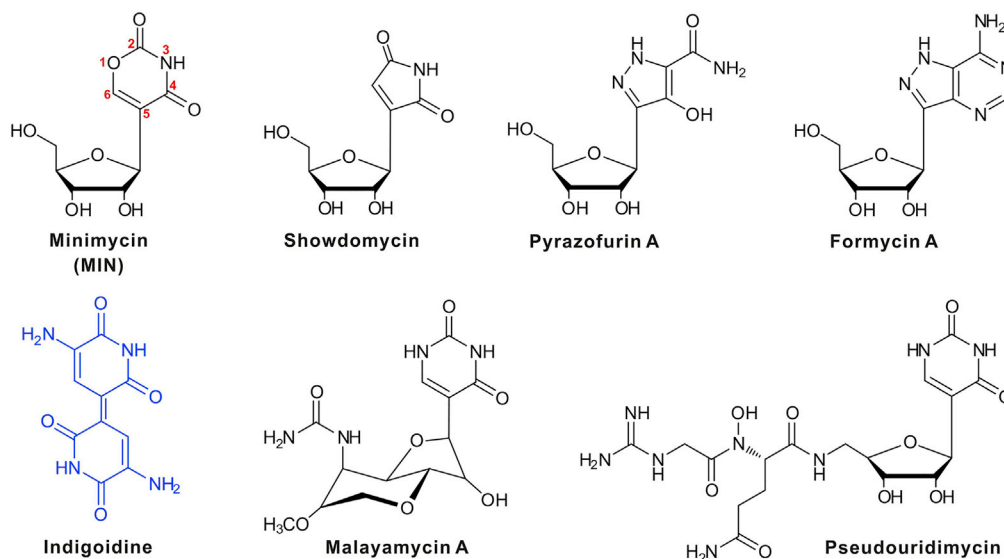


Figure 1. Chemical Structures of Representative C-Nucleoside Antibiotics and Indigoidine

Several C-nucleoside antibiotics (MIN-showdomycin, group I; pyrazofurin-formycin, group II; malayamycin-pseudouridimycin, group III) shown are deduced to employ distinct enzymatic logics for the assembly of the C-glycosidic bond. The structure of indigoidine is highlighted in blue to represent its intrinsic color.

(*idgS*) and a phosphopantetheinyl transferase gene (*sfp*) from surfactin biosynthesis (Nanjaraj Urs et al., 2019).

In the present study, we address the biosynthesis of C-nucleoside MIN and indigoidine in *Streptomyces hygroscopicus* JCM 4712. We report that a minimal 5-gene cluster is essential for MIN biosynthesis and show that the divergent biosynthesis of MIN and indigoidine is mediated by an NRPS, MinA. Moreover, we reveal that the N-terminal phosphatase domain of MinC (called MinC_N), the MinD uracil phosphoribosyltransferase, and the MinT transporter are safeguard enzymes, which collaboratively constitute an unusual self-resistance system, in which MinD likely employs an unprecedented substrate-competition strategy for self-resistance by increasing the UMP pool *in vivo*. Our deciphering of the C-nucleoside MIN pathway expands current understanding regarding natural product biosynthesis and self-resistance.

RESULTS AND DISCUSSION

Identification of MIN Biosynthetic Gene Cluster from *S. hygroscopicus* JCM 4712

To identify the gene cluster responsible for MIN biosynthesis, the genome of *S. hygroscopicus* JCM 4712 was sequenced using the Illumina HiSeq 4000 method, which renders 8.8-Mb data (G + C content 70.31%) after assembly of clean reads. MIN contains a C-glycosidic bond that is structurally similar to that of pseudouridine and showdomycin (Palmu et al., 2017) (Figure 1), implying that they should employ similar enzymatic logic for C-glycosidic bond formation. We therefore utilize pseudouridine 5'-phosphate glycosidase YeiN (GenBank: CAQ32570.1) and C-glycosynthase SdmA (GenBank: KKZ73237.1) as query sequences to conduct individual BLASTP analysis, leading to the discovery of two homologs ORF5178 (designated as MinB, 46%/49% identities to YeiN/SdmA) (Table 1) and ORF3816 (46%/46% identities to YeiN/SdmA) from the genome of *S. hygroscopicus* JCM 4712 (GenBank: MN397911). On the genomic region surrounding *minB* is a closely linked gene coding for a non-ribosomal peptide synthetase (MinA) (Figure 2A). The *orf3816* gene is linked with a kinase gene (GenBank: MN397911), which is identical to the YeiN-YeiC cascade for the pseudouridine metabolic pathway in *E. coli* (Preumont et al., 2008). These data suggest that the target region (*min*) covering *minA* and *minB* is likely to be involved in MIN biosynthesis.

To determine the identity of the *min* gene cluster, we directly cloned a ca. 11.2-kb region (likely housing the whole *min* gene cluster) using a two-step PCR strategy (Figure S1A; Tables S1 and S2). After confirmation (Figure S1B), the resultant plasmid pCHW301 was transferred into *Streptomyces coelicolor* M1154 (Gomez-Escribano and Bibb, 2014). The positive conjugants (*S. coelicolor* M1154::pCHW301) were then fermented

Protein	aa	Protein Function	Homolog, Origin	Identity, Similarity (%)	Accession No.
MinR	211	FadR family transcriptional regulator	SAMN05444521_6508, <i>Streptomyces</i> sp. 3124.6	87, 94	SHI26670
MinT	419	MFS transporter	SAMN05444521_6509, <i>Streptomyces</i> sp. 3124.6	79, 85	SHI26674
MinA	1379	NRPS(A-Ox-T-TE-Tau)	IndC, <i>S. chromofuscus</i> ATCC 49982	74, 82	AFV27434
MinB	317	C-glycosynthase	IndA, <i>S. chromofuscus</i> ATCC 49982	88, 93	AFV27435
MinC	613	HAD phosphatase and DUF4243 domain	IndB, <i>S. chromofuscus</i> ATCC 49982	77, 84	AFV27436
MinD	240	Uracil phosphoribosyltransferase	Orf2, <i>S. chromofuscus</i> ATCC 49982	81, 90	AFV27437

Table 1. Deduced Functions of the Open Reading Frames in the *min* Gene Cluster

for metabolite analysis. A bioassay indicated that the samples of M1154::pCHW301 show apparent inhibition against the indicator strain *Bacillus subtilis*, but the negative control (*S. coelicolor* M1154::pSET152) lacks related bioactivity (Figure S1C). High-performance liquid chromatography (HPLC) analysis showed that the sample of M1154::pCHW301 contains a new peak, which is absent from that of the negative control (Figure S1D). Further liquid chromatography-mass spectrometry (LC-MS) analysis shows that the LC peak is able to generate a characteristic $[M + H]^+$ ion at m/z 246.0609, with major fragment ions at m/z 155.9695, 210.1091, and 228.0699, fully consistent with the theoretical fragmentation pattern of MIN (Figures S1E–S1G).

To confirm the identity of the target metabolite accumulated by M1154::pCHW301, it was HPLC purified for 1D and 2D NMR analysis. As anticipated, the 1D NMR data of the target metabolite are closely matched to those of MIN (Figures S2A and S2B), and further detailed assignments of the compound as MIN are supported by ^1H - ^1H COSY (Correlation Spectroscopy) and HMBC (Heteronuclear Multiple Bond Correlation) spectra (Figures S2C and S2D). Analysis of the COSY NMR data led to the identification of a single isolated proton spin system corresponding to the ribose moiety (C-5', C-4', C-3', C-2', and C-1'), from which the relative configuration was determined based on the analysis of coupling constants. The connection between the ribose moiety and (2H)-1,3-oxazine-2,4-(3H)-dione subunit was deduced from HMBC correlations of H-6 with C-1'; H-1' with C-4 and C-6; and H-2' with C-5 (Table S3). Accordingly, the structure of the target metabolite was determined to be the same as that of MIN as shown. Taken together, these data demonstrate that the target gene cluster is responsible for the biosynthesis of MIN.

The Minimal 5-Gene (*minTABCD*) Cluster Is Essential for MIN Biosynthesis

In silico analysis revealed that the target 11.2-kb region (included in pCHW301) containing six genes is deduced to be involved in MIN biosynthesis. MinR shows 87% identity to SAMN05444521_6508 of *Streptomyces* sp. 3124.6, which is likely a FadR family transcriptional regulator. The second gene, *minT*, codes for an MFS transporter with high homology (79% identity) to SAMN05444521_6509 of *Streptomyces* sp. 3124.6 (Table 1), which is proposed to transport the antibiotic out of the producer cell. The *minA* product displays significant homology (74% identities in total) to IndC, an NRPS protein from *Streptomyces chromofuscus* ATCC 49982, and the domain architectures of both enzymes are highly matched (Table 1). MinB is shown to be homologous to IndA (pseudouridine-5'-phosphate glycosidase) with 88% identities (Table 1). Moreover, *in silico* analysis shows that MinC possesses 77% identities to IndB of *S. chromofuscus* ATCC 49982 (Table 1). Notably, *minC* encodes a 613-amino acid protein containing two domains, an N-terminal HAD phosphatase domain and the C-terminal DUF4243 domain with unassigned function. Concerning MinD, it shows 81% identity to Orf2 (uracil phosphoribosyltransferase) of *S. chromofuscus* ATCC 49982 (Table 1).

To precisely pinpoint the minimal gene cluster for MIN biosynthesis, we individually mutated the target genes by an *in vitro* CRISPR-Cas9 system (Liu et al., 2015). After confirmation (Figures S3A and S3B; Tables S2 and S4), the pCHW301 variants were conjugated into *S. coelicolor* M1154, and the resultant recombinants were fermented for further metabolite analysis. The antibacterial bioassay indicated that all the samples, with the exception for those of M1154::pCHW301 and M1154::pCHW301 Δ *minR*, lack bioactivities

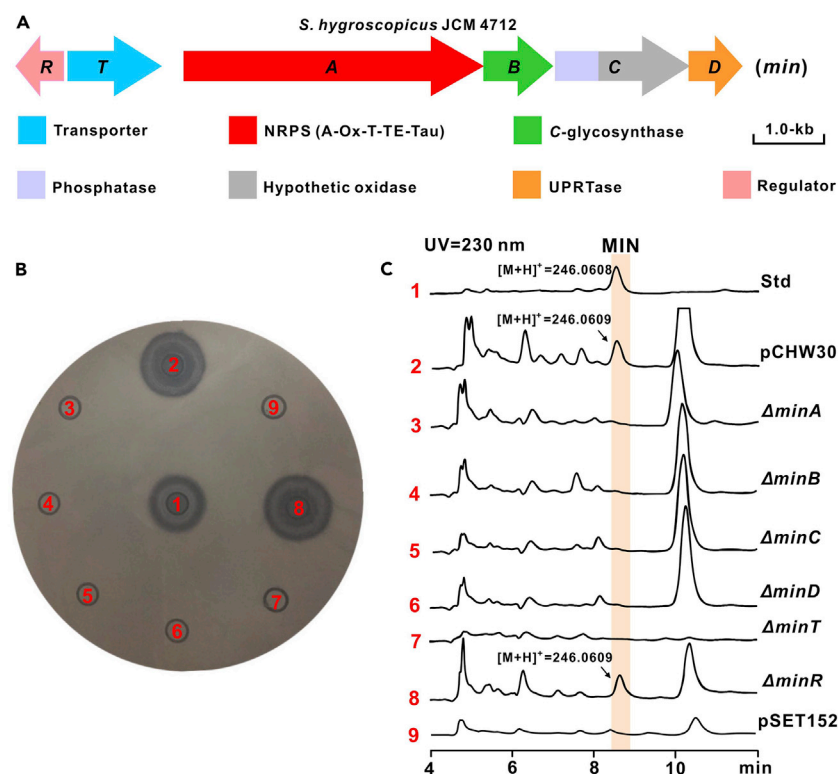


Figure 2. Genetic Organization and Investigation of the *min* Gene Cluster

(A) Genetic organization of the MIN gene cluster; A, adenylation domain; Ox, oxidase domain; T, thiolation domain; TE, thioesterase domain; Tau, tautomerase domain.

(B) Bioassays of the metabolites produced by related recombinants of *S. coelicolor* M1154. The indicator strain is *Bacillus subtilis*.

(C) HPLC analysis of the metabolites produced by related recombinants of *S. coelicolor* M1154. Std, the authentic standard of MIN; pCHW301, the metabolites of the recombinant *S. coelicolor* M1154 containing pCHW301; $\Delta minA$, the metabolites of the recombinant *S. coelicolor* M1154 containing pCHW301 $\Delta minA$, and other samples are correspondingly assigned; pSET152, the metabolites of the recombinant *S. coelicolor* M1154 containing pSET152 as negative control. The aliphatic numbers correspond to those in the bioassay plate.

See also Figures S1–S3; Tables 1 and S1–S4.

against the *Bacillus subtilis* indicator strain (Figure 2B). Moreover, reverse-phase HPLC analysis indicated that the sample from M1154::pCHW301 $\Delta minR$ could also produce the distinctive peak for MIN (Figure 2C), whose identity was further confirmed by LC-MS analysis (Figures S3C–S3F), suggesting that MIN biosynthesis is not under strict regulation by *minR* in *S. coelicolor*. These data demonstrate that a minimal 5-gene cluster (*minTABCD*) is essential for the maintenance of MIN biosynthesis.

Reconstitution of the MinA-Mediated Pathway for Indigoidine Biosynthesis

Bioinformatic analysis showed that MinA is a typical NRPS protein containing multiple A-Ox-T-TE-Tau domains (Figure S4A; Table 1). More surprisingly, MinA homologs had been previously characterized as the indigoidine synthetases (Takahashi et al., 2007) (Figure 3A), and we were therefore curious about how this enzyme is utilized to build MIN. To evaluate the functional role of MinA, the *minA* sequence was optimized on the basis of *E. coli* preference (Table S5), and the resultant plasmid pET28a/*minA** (*signifies the optimized sequence) was transferred into *E. coli* for protein overexpression and metabolite analysis. As anticipated, the broth of the *E. coli* recombinant showed a distinctive blue color (indigo) (Figure 3B), implicating the potential production of indigo dye. To further determine the identity of the blue pigment, a metabolite sample from the *E. coli* pET28a/*minA** was submitted for HPLC assessment, generating a characteristic peak that was absent from the *E. coli* strain lacking *minA** (negative control) (Figures 3B, S4B, and S4C). Further LC-MS analysis indicated that the LC peak produces an $[M + H]^+$ ion at m/z 249.0615, and corresponding fragment ions at m/z 216.7811 and 231.9472, consistent with those of indigoidine (Figures S4D

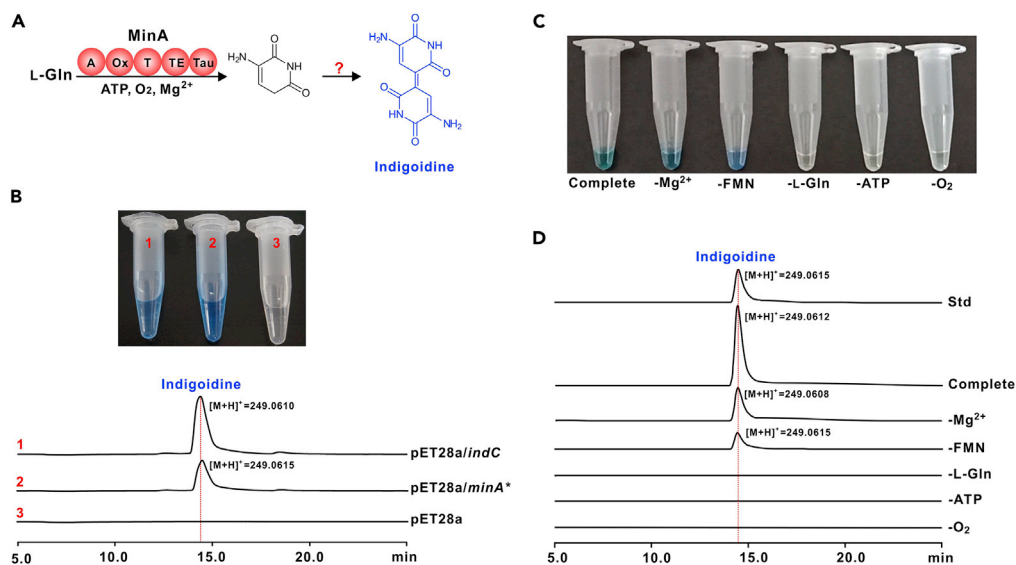


Figure 3. In Vivo and In Vitro Reconstitution of the MinA Mediated Assembly Line

(A) Schematic of the MinA-mediated assembly line for indigoidine biosynthesis.
 (B) Engineered production of indigoidine in *E. coli*. Top, the target metabolite (blue) produced by related strains. Bottom, HPLC analysis of the target metabolite indigoidine produced by related *E. coli* strains. pET28a/*indC*, extracted metabolite of *E. coli* BAP1 containing *indC* (indigoidine synthetase gene from *S. chromofuscus* ATCC 49982) as positive control; pET28a/*minA*^{*}, extracted metabolite of *E. coli* BAP1 containing *minA*^{*}; pET28a, extracted metabolite of *E. coli* BAP1 containing pET28a as negative control.
 (C) The extracted enzymatic products of the MinA reactions. Complete, the MinA reaction with all essential factors added; -Mg²⁺, the MinA reaction without adding exogenous Mg²⁺; -FMN, the MinA reaction without adding exogenous FMN; -L-Gln, the MinA reaction without L-glutamine added; -ATP, the MinA reaction without ATP added; -O₂, the MinA reaction under N₂ atmosphere.
 (D) HPLC analysis of the related MinA reactions. The characteristic [M + H]⁺ ion of indigoidine was also indicated on this panel, and the information for related samples corresponds to that in panel C.
 See also [Figures S4](#) and [S5](#); [Tables S1](#) and [S5](#).

and S4E). Hence, this demonstrated that the single NRPS (MinA)-mediated pathway is sufficient to support indigoidine biosynthesis.

To reconstitute MinA activity *in vitro*, we over-expressed and purified the MinA protein from *E. coli*. The purified MinA shows bright yellow color ([Figures S4F](#) and [S4G](#)), a typical feature of a flavin-dependent protein, as confirmed by LC-MS analysis ([Figures S4H](#) and [S4I](#)). Enzymatic assays with the recombinant MinA produced an obvious blue color, implicating the production of indigoidine ([Figures 3C](#) and [3D](#)), whose identity is further confirmed by LC-MS analysis ([Figure S4J](#)). The *in vitro* reaction without enzyme added (negative control) was unable to generate the blue-colored product, and the enzyme reactions in the absence of L-glutamine, ATP, or O₂ also generate similar negative results ([Figure 3D](#)). Furthermore, the purified MinA has only partial activity without an exogenous addition of FMN or Mg²⁺ ([Figures 3D](#) and [S4K–S4M](#)) and indicates the preference to relative low temperatures (18°C of all temperatures tested) ([Figures S4N–S4P](#) and [S4R](#)). Subsequently, we tested the substrate flexibility for MinA against the unnatural isomer D-glutamine with negative result ([Figures S4Q](#) and [S4R](#)). These combined data substantially established that divergent biosynthesis of MIN and indigoidine is mediated by the NRPS (MinA) pathway, in which the compound **1** is likely converted to indigoidine via a non-enzymatic spontaneous reaction.

The potential pathways mediated by MinA homologs, as shown by *in silico* analysis, are actually more widely distributed than we initially imagined. In addition, there is also a high degree of diversity at the genetic level ([Figure S5](#)). Earlier studies reported that indigoidine production affects the pathogenicity of the plant pathogen *Dickeya dadantii* ([Reverchon et al., 2002](#)). In the present study, we tentatively propose that this bacterium could perform its pathogenic role by the coupled production of a potential MIN-related compound ([Figure S5](#)), and it is of great interest for future study to elucidate such pathogenic mechanism at the molecular level.

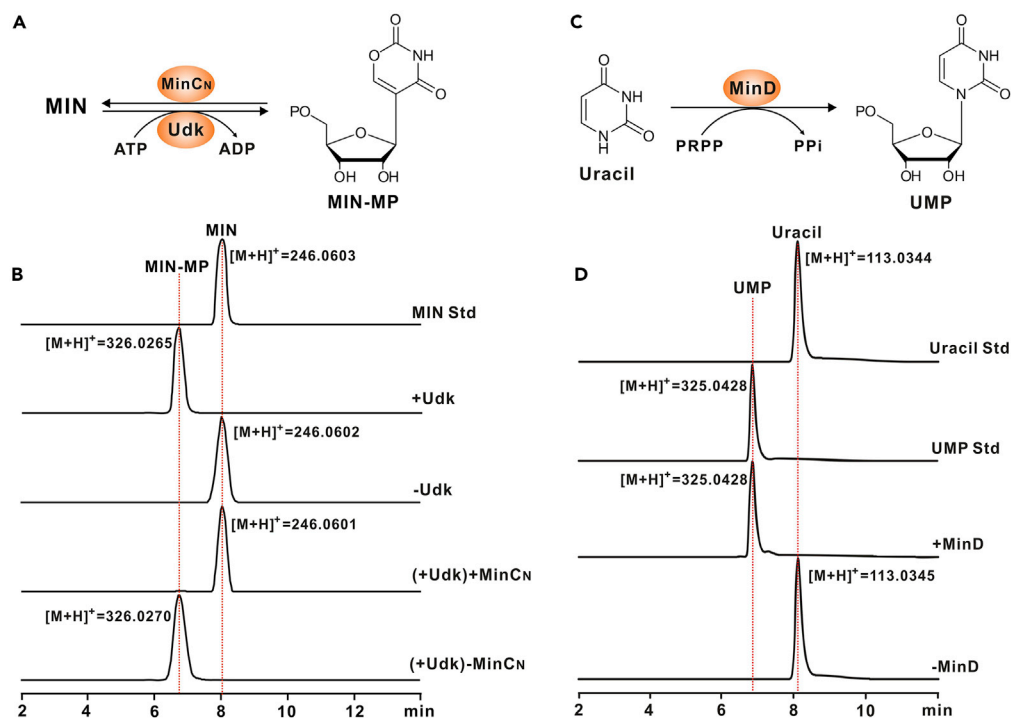


Figure 4. Functional Characterization of MinC_N/MinD as Phosphatase/UPRTase

(A) Schematic of MinC_N-catalyzed reaction. Udk, uridine kinase (GenBank: QBJ70019.1) from *Bacillus subtilis*; MIN-5'-MP, MIN-5'-monophosphate.

(B) LC-HRMS analysis of the Udk/MinC_N reactions. MIN Std, the authentic standard of MIN; +Udk, the Udk catalyzed reaction to form MIN-MP; -Udk, the reaction without Udk added as negative control; (+Udk)+MinC_N, the Udk reaction, proceeded for 4 h, with further addition of MinC_N for another 1 h; (+Udk)-MinC_N, the Udk reaction (proceeded for 4 h) without further addition of MinC_N (also incubated for another 1 h). The characteristic [M + H]⁺ ions of MIN and MIN-MP are indicated as well in this panel for related peaks.

(C) Schematic of MinD-catalyzed reaction. PRPP, phosphoribosyl pyrophosphate.

(D) HPLC traces of the MinD reactions. Uracil Std, the authentic standard of uracil; UMP Std, the authentic standard of UMP; +MinD, the MinD reaction using uracil and PRPP as substrates; -MinD, the reaction without MinD added as negative control. The characteristic [M + H]⁺ ions of UMP/uracil are also indicated in this panel.

See also Figures S6 and S7; Tables S1 and S6.

MinC_N Is Responsible for the Final Dephosphorylation Step, and MinD Functions as a Uracil Phosphoribosyltransferase (UPRTase)

In silico analysis showed that MinC is a two-domain enzyme, consisting of an N-terminal phosphatase domain and a C-terminal domain of undefined function (we have not yet determine the characteristic properties of MinC_C in the present study) (Figures S6A and S6B), and that in some cases these are separated into two independent proteins (Figure S6A). To determine if MinC_N catalyzes the final dephosphorylation step (Figure 4A), we over-expressed and purified the protein from *E. coli* to near homogeneity (Figure S6C). This was assayed *in vitro* against the substrate MIN-MP, which is supplied by the Udk (uridine kinase from *Bacillus subtilis*, GenBank: QBJ70019.1) (Table S6)-catalyzed reaction (Figures S6D–S6H). LC-MS analysis of the *in vitro* reaction products indicated that the MinC_N reaction is capable of generating a characteristic [M + H]⁺ ion at *m/z* 246.0601, with major fragment ions at *m/z* 155.9384, 210.1541, and 228.0651, consistent with those of the authentic MIN standard (Figures 4B and S6I–S6K). This characteristic MIN peak was absent from the reaction without MinC_N added (Figures 4B and S6L). Hence, these data support the hypothesis that MinC_N is responsible for the final dephosphorylation step during MIN biosynthesis.

Bioinformatic analysis suggested that *minD* encodes an UPRTase, which are generally involved in the pyrimidine salvage pathway by catalyzing the reaction between uracil and phosphoribosylpyrophate (PRPP) to regenerate UMP (Singh et al., 2015) (Figures 4C and S7A). To investigate the enzymatic role of MinD, it was over-expressed and purified from *E. coli* (Figure S7B), and the corresponding activity was determined *in vitro*. As anticipated,

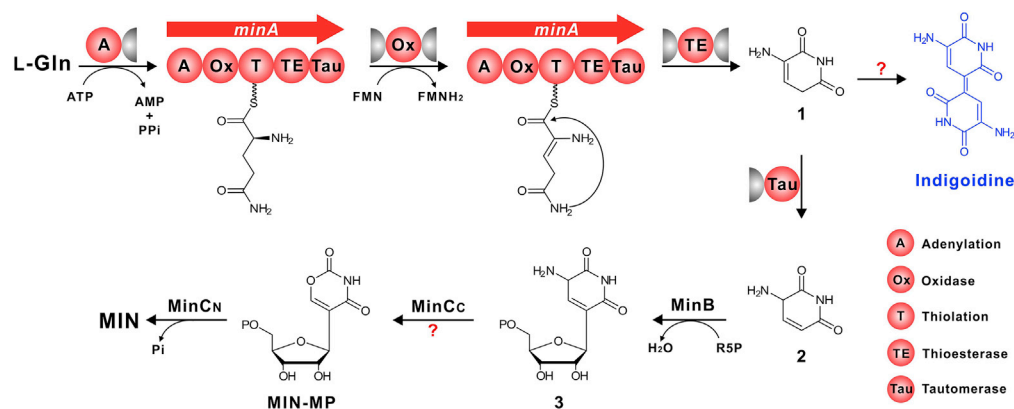


Figure 5. Proposed Pathway for the Biosynthesis of MIN and Indigoidine

Proposed pathway for the divergent biosynthesis of MIN and indigoidine. See also Figure S5.

HPLC analysis showed that the MinD-catalyzed reaction could generate a peak for UMP, corresponding to an authentic standard, which was absent from the negative control (Figure 4D). Further LC-MS analysis indicated that the target peak gave rise to a characteristic $[M + H]^+$ ion for UMP at m/z 325.0428, and main fragment ions at m/z 212.9202 and 227.0645, completely consistent with those of the UMP authentic standard (Figures S7C–S7E). These results establish that MinD functions as an UPRTase for the synthesis of UMP.

Divergent Biosynthesis of MIN and Indigoidine Is Mediated by an NRPS-Associated Assembly Line

Previous isotopic feeding experiments had showed that L-glutamate is incorporated into the oxazine ring of MIN (Isono and Suhadolnik, 1977; Suhadolnik and Reichenbach, 1981), whereas its ribosyl moiety is from D-ribose (Isono and Suhadolnik, 1975). In the present work, this mechanism is shown to be reasonable. MIN biosynthesis is confirmed to be initiated by MinA, which specifically selects L-glutamine as substrate, and the tethered amino acid is then dehydrogenated under strict and precise stereospecificity/regiospecificity at the C2–C3 positions by the oxidase domain (Ox domain). Subsequently, compound 1 is released by hydrolysis of the TE domain. Compound 1, as a key branch intermediate, is proposed to be converted to indigoidine by a spontaneous oxidative coupling reaction (Figure 5). Simultaneously, this intermediate could be tautomerized by the Tau domain to form 2, which is modified by the MinB C-glycosynthase to produce 3. Compound 3 subsequently undergoes an unusual oxidative deamination and recombination reaction catalyzed by MinC_C to generate MIN-MP, which is followed by the final dephosphorylation step to complete MIN biosynthesis (Figure 5). MinC_C features a DUF4243 domain, which is also present in a Baeyer-Villiger oxidase AflyY of the aflatoxin biosynthetic pathway (Ehrlich et al., 2005). In this respect, MinC_C represents a novel type of Baeyer-Villiger oxidase catalyzing an unprecedented and intriguing oxidative deamination and recombination reaction, and relevant studies to investigate its enzymatic logic are now underway in our laboratory.

Indigoidine is a well-established microbial metabolite known for over half a century. However, it has now been established for the first time that this pigment is actually associated with the co-production of the C-nucleoside MIN. Accordingly, it is possible that indigoidine biosynthesis from an increasing number of potential pathways may be associated with related unknown C-nucleoside molecules, because analogs of the MinA–MinB pair are in several cases concomitantly present in the specific gene clusters (Figure S5). L-glutamate is the common precursor for the aglycon of the C-nucleoside antibiotics, including MIN, formycin, pyrazofurin, and showdomycin (Suhadolnik and Reichenbach, 1981), which until recently have been unexplored at the molecular level (Hong et al., 2019; Palmu et al., 2017; Sosio et al., 2018; Wang et al., 2019). Hence, we propose that further insight into the molecular logics underlying the biosynthesis of C-nucleoside antibiotics will identify diverse and unique enzymes for potential synthetic biology purposes.

MinC_N, MinD, and MinT Functioning as the Safeguard Enzymes Constitute a Collaborative Self-Resistance System during MIN Biosynthesis

The assignment of MinD as a UPRTase raises an interesting open question: what is the functional role of this enzyme during MIN biosynthesis? Considering the fact that MIN is also active against *Streptomyces*, we

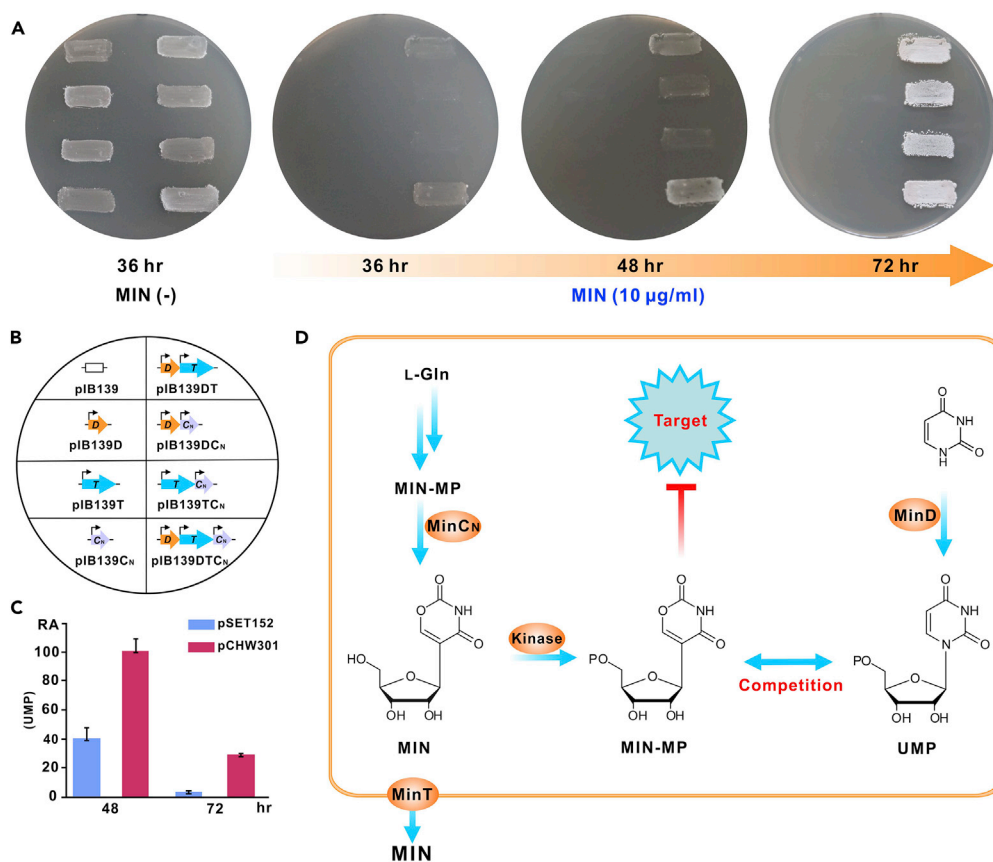


Figure 6. Proposed Self-Resistance Mechanism for the Biosynthesis of MIN

(A) Plate-grown experiments for *S. coelicolor* M1154 recombinants containing related genes. For the first two plates, the recombinant incubated for 36 h (in the related square) corresponds to each other. For plates 2–4, it means the identical plate that was incubated for different time (marker at the bottom of each plate); MIN (-), the MIN-negative plate; MIN (10 µg/mL), the plate containing MIN at a final concentration of 10 µg/mL. The recombinant in the related square corresponds to that described as below.

(B) Representational map for the plate-grown experiments. piB139, *S. coelicolor* M1154 containing the empty vector piB139; piB139D, *S. coelicolor* M1154 containing piB139/*minD*; piB139T, *S. coelicolor* M1154 containing piB139/*minT*; piB139C_N, *S. coelicolor* M1154 containing piB139/*minC_N*; piB139DT, *S. coelicolor* M1154 containing piB139/*minDT*; piB139DC_N, *S. coelicolor* M1154 containing piB139/*minDC_N*; piB139TC_N, *S. coelicolor* M1154 containing piB139/*minTC_N*; piB139DTC_N, *S. coelicolor* M1154 containing piB139/*minDTC_N*.

(C) The relative abundance of the UMP concentrations *in vivo* for the strains at different growth stages (48 and 72 h). pSET152, the sample of *S. coelicolor* M1154::pSET152 (blue); pCHW301, the sample of *S. coelicolor* M1154::pCHW301 (red); "RA" denotes relative abundance. Data are represented as mean ± SEM.

(D) Proposed collaborative self-resistance system during MIN biosynthesis. Three enzymes, including MinC_N, MinT, and MinD, collaborate to fulfill the mission of self-resistance during MIN biosynthesis, and MinD, acting as the key safeguard enzyme, employs an unprecedented strategy of substrate competition to achieve self-resistance during MIN biosynthesis.

See also Figure S7 and Table S1.

tentatively propose that it may play a key role in self-resistance during MIN biosynthesis by employing an unprecedented mechanism. We therefore introduced *minD* into *S. coelicolor* M1154 to determine whether it mediates a safeguard role. In contrast to this expectation, the recombinant strain (M1154::piB139*minD*) had no apparent resistance to MIN (10 µg/mL). Accordingly, we re-examined the MIN gene cluster and noticed that *minC_N* and *minT* are also potential contributors to the self-resistance system. To test the assumption, we individually introduced these two genes into *S. coelicolor* M1154. However, neither gene was capable of supporting the growth of the corresponding *S. coelicolor* M1154 recombinants in the presence of MIN (10 µg/mL, the minimal inhibitory concentration against *S. coelicolor* M1154-derived negative controls in this study) (Figures 6A and 6B).

These results suggested that some combination of *minC_N*, *minD*, and *minT* may collaborate to fulfill the self-resistance role, and we accordingly introduced these different combinations into *S. coelicolor* M1154. Notably, several of these combinations are able to support the effective growth of the corresponding *S. coelicolor* M1154 recombinants in the presence of MIN, whereas the introduced single *minC_N*, *minD*, or *minT* could not maintain the apparent growth of the related recombinants. It was also observed that *minD* has a greater contribution to the self-resistance system, and the combination (containing *minC_N*, *minD*, and *minT*) could maintain the optimal growth status for the counterpart recombinant (Figures 6A and 6B). Together, these data demonstrate that *minD*, in collaboration with *minC_N* and *minT*, determines the functional role *in vivo* constituting the self-resistance system during MIN biosynthesis.

Biosynthesis of MIN Employs a Substrate-Competition Strategy for Self-Resistance

A further relevant question is how MIN executes its inhibitory role *in vivo*? We propose that similar to many other nucleoside analogs (Jordheim et al., 2013), the phosphorylated form (MIN-MP) of MIN functions as the active inhibitory molecule. This is also supported by the discovery of kinases (from *S. coelicolor* M1154 and *Bacillus subtilis*) capable of recognizing MIN as substrates (Figures S6C–S6H), and the fact that MinD (UPRTase) may function as a safeguard enzyme by enhancing the *in vivo* UMP pool of microbial cells. To test this suggestion, we conducted bioassays using *Bacillus subtilis* as an indicator strain by exogenous addition of uridine and MIN at different concentration ratios. This strain showed resistance to MIN in the co-presence of relative high concentration of uridine (Figure S7F), implying that uridine, which is efficiently metabolized to UMP *in vivo*, is capable of partly alleviating the inhibition of MIN. Moreover, the *in vivo* UMP concentrations for the *S. coelicolor* M1154 recombinants, as determined by LC-high-resolution MS (HRMS), are considerably higher than those of the negative control (*S. coelicolor* M1154::pSET152) (Figures 6C and S7G), providing further support for the self-resistance model employed in MIN biosynthesis. In contrast, the *in vivo* MIN-MP (the active form of MIN), as indicated by LC-HRMS, is undetectable due to the relatively much lower concentration (if compared with that of UMP) (Figures S7H and S7I). These data support the hypothesis that the inhibitory role of MIN is attenuated by UMP by an unprecedented substrate-competition mechanism.

Biosynthetic bacteria have evolved several strategies for self-resistance during natural product production, often transporting the metabolite out of the producer cell upon its synthesis, or by modification of natural products or the target site (Wencewicz, 2019). The substrate-competition strategy for self-resistance presented here is, to the best of our knowledge, unique, but it may be broadly exploited for microbial natural products biosynthesis. In this self-resistance system, the active inhibitory molecule MIN-MP is immediately dephosphorylated to form the end product MIN, most of which will be promptly transported out of the producer cells. MinD, therefore, functions as a safeguard enzyme that responds to sub-inhibitory concentrations of MIN-MP by increasing the UMP pool *in vivo*, thereby achieving the self-resistance for the producer cell (Figure 6D).

Limitations of the Study

In this study, we have uncovered that divergent biosynthesis of MIN and indigoidine is mediated by an NRPS enzyme and have demonstrated that an unprecedented collaborative self-resistance system is employed for MIN biosynthesis. However, the precise mechanism of how MIN executes its inhibitory role will require further study. Further studies will also be required to understand the enzymatic formation of the oxazine ring substituent of MIN.

METHODS

All methods can be found in the accompanying [Transparent Methods supplemental file](#).

DATA AND CODE AVAILABILITY

The DNA sequence is deposited in the GenBank database under individual accession numbers MK122964 (for the *min* gene cluster from *S. hygroscopicus* JCM 4712) and MN397911 (for the genes *orf3815* and *orf3816* from *S. hygroscopicus* JCM 4712).

SUPPLEMENTAL INFORMATION

Supplemental Information can be found online at <https://doi.org/10.1016/j.isci.2019.11.037>.

ACKNOWLEDGMENTS

We are grateful to Prof. Jixun Zhan (Utah State University, USA) for kindly providing us with related research material. This work was supported by grants National Key R & D Program of China (2018YFA0903203), the National Natural Science Foundation of China (31770041, 31970052), and the foundation of Tianjin Engineering Research Center of Microbial Metabolism and Fermentation Process Control, China (ZXKF20180202).

AUTHOR CONTRIBUTIONS

L.K., G.X., X.L., J.W., and Z.T. conducted the genetic and biochemical experiments. W.T. helped with the preparation of figures. Y.-S.C. and K.S. analyzed the NMR data. W.C. conceived the project and directed the research. W.C. wrote the manuscript, and Y.Z., Z.D., and N.P.J.P. made a critical reading of the manuscript.

DECLARATION OF INTERESTS

The authors declare no competing interests.

Received: September 11, 2019

Revised: November 13, 2019

Accepted: November 19, 2019

Published: December 20, 2019

REFERENCES

- Brown, A.S., Robins, K.J., and Ackerley, D.F. (2017). A sensitive single-enzyme assay system using the non-ribosomal peptide synthetase BpsA for measurement of L-glutamine in biological samples. *Sci. Rep.* 7, 41745.
- De Bernardo, S., and Weigele, M. (1977). Synthesis of oxazinomycin (minimycin). *J. Org. Chem.* 42, 109–112.
- Ehrlich, K.C., Montalbano, B., Boue, S.M., and Bhatnagar, D. (2005). An aflatoxin biosynthesis cluster gene encodes a novel oxidase required for conversion of versicolorin A to sterigmatocystin. *Appl. Environ. Microbiol.* 71, 8963–8965.
- Gomez-Escribano, J.P., and Bibb, M.J. (2014). Heterologous expression of natural product biosynthetic gene clusters in *Streptomyces coelicolor*: from genome mining to manipulation of biosynthetic pathways. *J. Ind. Microbiol. Biotechnol.* 41, 425–431.
- Heumann, W., Young, D., and Gottlich, C. (1968). Leucoindigoidine formation by an *Arthrobacter* species and its oxidation to indigoidine by other micro-organisms. *Biochim. Biophys. Acta* 156, 429–431.
- Hong, H., Samborsky, M., Zhou, Y., and Leadlay, P.F. (2019). C-nucleoside formation in the biosynthesis of the antifungal malayamycin A. *Cell Chem. Biol.* 26, 493–501.e5.
- Isono, K. (1988). Nucleoside antibiotics: structure, biological activity, and biosynthesis. *J. Antibiot. (Tokyo)* 41, 1711–1739.
- Isono, K., and Suhadolnik, R.J. (1975). The biosynthesis of the nucleoside antibiotics: minimycin formation by *Streptomyces hygroscopicus*. *Ann. N. Y. Acad. Sci.* 255, 390–401.
- Isono, K., and Suhadolnik, R.J. (1977). Biosynthesis of the C-nucleoside, minimycin: asymmetric incorporation of glutamate and acetate into the oxazine ring. *J. Antibiot. (Tokyo)* 30, 272–273.
- Jordheim, L.P., Durantel, D., Zoulim, F., and Dumontet, C. (2013). Advances in the development of nucleoside and nucleotide analogues for cancer and viral diseases. *Nat. Rev. Drug Discov.* 12, 447–464.
- Kuhn, R., Starr, M.P., Kuhn, D.A., Bauer, H., and Knackmuss, H.J. (1965). Indigoidine and other bacterial pigments related to 3,3'-Bipyridyl. *Arch. Mikrobiol.* 51, 71–84.
- Kusakabe, Y., Nagatsu, J., Shibuya, M., Kawaguchi, O., and Hirose, C. (1972). Minimycin, a new antibiotic. *J. Antibiot. (Tokyo)* 25, 44–47.
- Li, X.Y., Ma, S.Q., and Yi, C.Q. (2016). Pseudouridine: the fifth RNA nucleotide with renewed interests. *Curr. Opin. Chem. Biol.* 33, 108–116.
- Liu, Y., Tao, W., Wen, S., Li, Z., Yang, A., Deng, Z., and Sun, Y. (2015). *In Vitro* CRISPR/Cas9 System for efficient targeted DNA editing. *MBio* 6, e01714–01715.
- Maffioli, S.I., Zhang, Y., Degen, D., Carzaniga, T., Del Gatto, G., Serina, S., Monciardini, P., Mazzetti, C., Guglielame, P., Candiani, G., et al. (2017). Antibacterial nucleoside-analog inhibitor of bacterial RNA polymerase. *Cell* 169, 1240–1248.e23.
- Muller, M., Auslander, S., Auslander, D., Kemmer, C., and Fussenegger, M. (2012). A novel reporter system for bacterial and mammalian cells based on the non-ribosomal peptide indigoidine. *Metab. Eng.* 14, 325–335.
- Nanjaraj Urs, A.N., Hu, Y., Li, P., Yuchi, Z., Chen, Y., and Zhang, Y. (2019). Cloning and expression of a nonribosomal peptide synthetase to generate blue rose. *ACS Synth. Biol.* 8, 1698–1704.
- Novakova, R., Odnogova, Z., Kutas, P., Feckova, L., and Kormanec, J. (2010). Identification and characterization of an indigoidine-like gene for a blue pigment biosynthesis in *Streptomyces aureofaciens* CCM 3239. *Folia Microbiol. (Praha)* 55, 119–125.
- Olano, C., Garcia, I., Gonzalez, A., Rodriguez, M., Rozas, D., Rubio, J., Sanchez-Hidalgo, M., Brana, A.F., Mendez, C., and Salas, J.A. (2014). Activation and identification of five clusters for secondary metabolites in *Streptomyces albus* J1074. *Microb. Biotechnol.* 7, 242–256.
- Pait, I.G.U., Kitani, S., Kurniawan, Y.N., Asa, M., Iwai, T., Ikeda, H., and Nihira, T. (2017). Identification and characterization of lbpA, an indigoidine biosynthetic gene in the gamma-butyrolactone signaling system of *Streptomyces lavendulae* FRI-5. *J. Biosci. Bioeng.* 124, 369–375.
- Palmu, K., Rosenqvist, P., Thapa, K., Iilina, Y., Siitonen, V., Baral, B., Mäkinen, J., Belogurov, G., Virta, P., Niemi, J., et al. (2017). Discovery of the showdomycin gene cluster from *Streptomyces showdoensis* ATCC 15227 yields insight into the biosynthetic logic of C-nucleoside antibiotics. *ACS Chem. Biol.* 12, 1472–1477.
- Preumont, A., Snoussi, K., Stroobant, V., Collet, J.F., and Van Schaftingen, E. (2008). Molecular identification of pseudouridine-metabolizing enzymes. *J. Biol. Chem.* 283, 25238–25246.
- Reverchon, S., Rouanet, C., Expert, D., and Nasser, W. (2002). Characterization of indigoidine biosynthetic genes in *Erwinia chrysanthemi* and role of this blue pigment in pathogenicity. *J. Bacteriol.* 184, 654–665.
- Rezuchova, B., Homerova, D., Sevcikova, B., Nunez, L.E., Novakova, R., Feckova, L., Skultety, L., Cortes, J., and Kormanec, J. (2018). An efficient

blue-white screening system for markerless deletions and stable integrations in *Streptomyces chromosomes* based on the blue pigment indigoidine biosynthetic gene *bpsA*. *Appl. Microbiol. Biotechnol.* **102**, 10231–10244.

Sasaki, K., Kusakabe, Y., and Esumi, S. (1972). The structure of minimycin, a novel carbon-linked nucleoside antibiotic related to β -pseudouridine. *J. Antibiot. (Tokyo)* **25**, 151–154.

Singh, V., Brecik, M., Mukherjee, R., Evans, J.C., Svetlikova, Z., Blasko, J., Surade, S., Blackburn, J., Warner, D.F., Mikusova, K., et al. (2015). The complex mechanism of antimycobacterial action of 5-fluorouracil. *Chem. Biol.* **22**, 63–75.

Sosio, M., Gaspari, E., Iorio, M., Pessina, S., Medema, M.H., Bernasconi, A., Simone, M., Maffioli, S.I., Ebright, R.H., and Donadio, S. (2018). Analysis of the pseudouridimycin biosynthetic pathway provides insights into the formation of C-nucleoside antibiotics. *Cell Chem. Biol.* **25**, 540–549.e4.

Starr, M.P., Cosens, G., and Knackmuss, H.J. (1966). Formation of the blue pigment indigoidine by phytopathogenic erwinia. *Appl. Microbiol.* **14**, 870–872.

Suhadolnik, R.J., and Reichenbach, N.L. (1981). Glutamate as the common precursor for the aglycon of the naturally occurring C-nucleoside antibiotics. *Biochemistry* **20**, 7042–7046.

Takahashi, H., Kumagai, T., Kitani, K., Mori, M., Matoba, Y., and Sugiyama, M. (2007). Cloning and characterization of a *Streptomyces* single module type non-ribosomal peptide synthetase catalyzing a blue pigment synthesis. *J. Biol. Chem.* **282**, 9073–9081.

Tymiak, A.A., Culver, C.A., Goodman, J.F., Seiner, V.S., and Sykes, R.B. (1984). Oxazinomycin produced by a *Pseudomonas* species. *J. Antibiot. (Tokyo)* **37**, 416–418.

Wang, S.A., Ko, Y., Zeng, J., Geng, Y., Ren, D., Ogasawara, Y., Irani, S., Zhang, Y., and Liu, H.W.

(2019). Identification of the formycin A biosynthetic gene cluster from *Streptomyces kaniharaensis* illustrates the interplay between biological pyrazolopyrimidine formation and de novo purine biosynthesis. *J. Am. Chem. Soc.* **141**, 6127–6131.

Wencewicz, T.A. (2019). Crossroads of antibiotic resistance and biosynthesis. *J. Mol. Biol.* **431**, 3370–3399.

Xie, Z., Zhang, Z., Cao, Z., Chen, M., Li, P., Liu, W., Qin, H., Zhao, X., Tao, Y., and Chen, Y. (2017). An external substrate-free blue/white screening system in *Escherichia coli*. *Appl. Microbiol. Biotechnol.* **101**, 3811–3820.

Yu, D., Xu, F., Valiente, J., Wang, S., and Zhan, J. (2013). An indigoidine biosynthetic gene cluster from *Streptomyces chromofuscus* ATCC 49982 contains an unusual IndB homologue. *J. Ind. Microbiol. Biotechnol.* **40**, 159–168.

ISCI, Volume 22

Supplemental Information

Divergent Biosynthesis of C-Nucleoside

Minimycin and Indigoidine in Bacteria

Liyuan Kong, Gudan Xu, Xiaoqin Liu, Jingwen Wang, Zenglin Tang, You-Sheng Cai, Kun Shen, Weixin Tao, Yu Zheng, Zixin Deng, Neil P.J. Price, and Wenqing Chen

1. Supplementary Figures

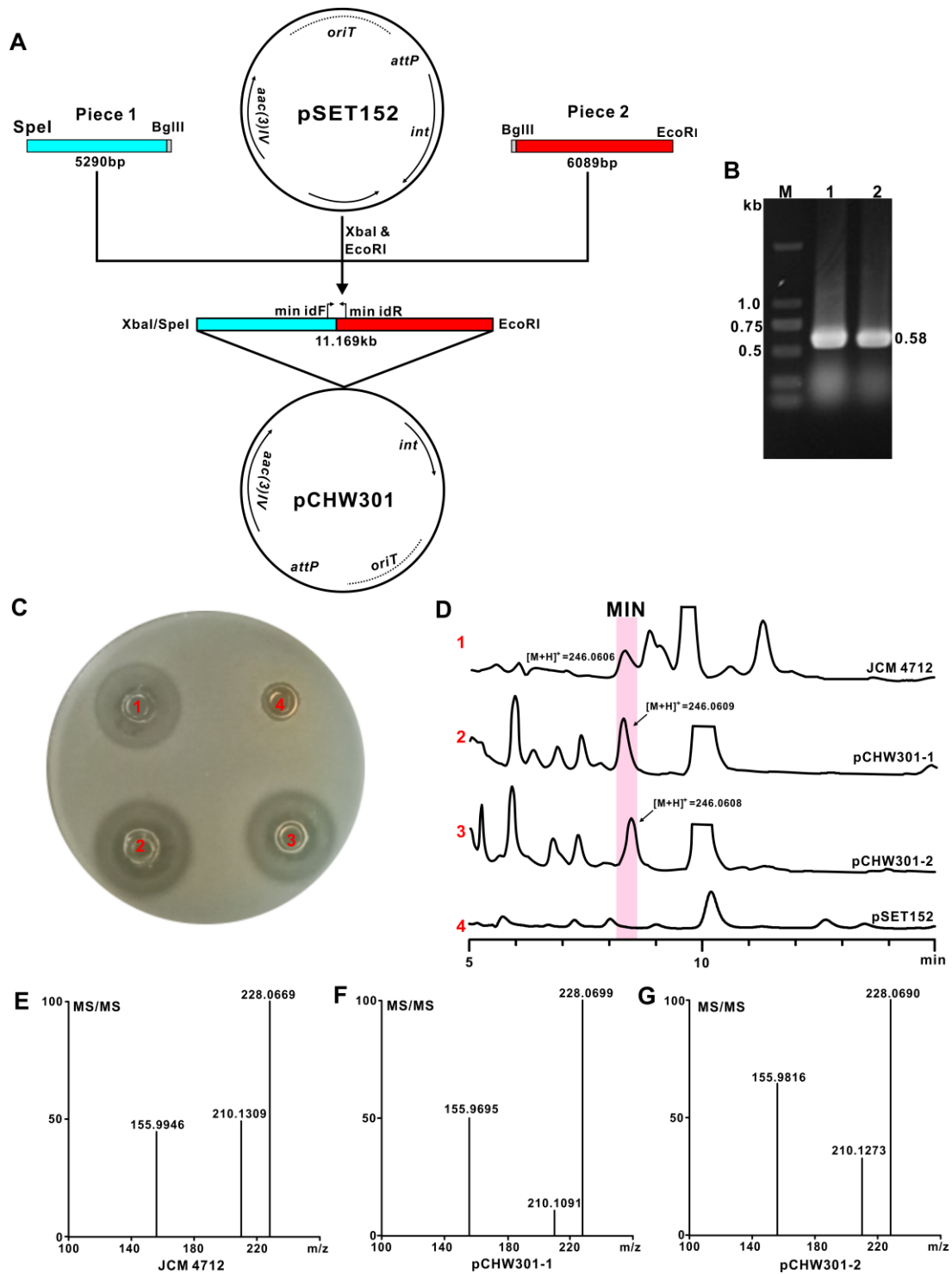


Figure S1. Direct cloning and heterologous expression of the *min* gene cluster, Related to Figure 2.

(A) Representational map for the construction of pCHW301. (B) PCR identification of the positive plasmid containing *min* gene cluster. M, DM2000 ladder (ComWin

Biotech); 1, PCR product (positive control) using genomic DNA of *S. hygrosopicus* JCM 4712 as template; 2, PCR product using the positive plasmid (pCHW301) as template. (C) Bioassay of the metabolites produced by related strains. 1, the fermentation broth of *S. hygrosopicus* JCM 4712; 2, the fermentation broth of *S. coelicolor* M1154::pCHW301-1; 3, the fermentation broth of *S. coelicolor* M1154::pCHW301-2; 4, the fermentation broth of *S. coelicolor* M1154::pSET152. (D) HPLC analysis of the metabolites produced by related strains. JCM 4712, the sample of *S. hygrosopicus* JCM 4712; pCHW301-1, the sample of *S. coelicolor* M1154::pCHW301-1; pCHW301-2, the sample of *S. coelicolor* M1154::pCHW301-2; pSET152, the sample of *S. coelicolor* M1154::pSET152 as negative control. (E-G) HRMS/MS analysis of the target product produced by related strains. As shown in this panel, the individual HRMS/MS analysis of the target product corresponds to that in panel D (shadow region).

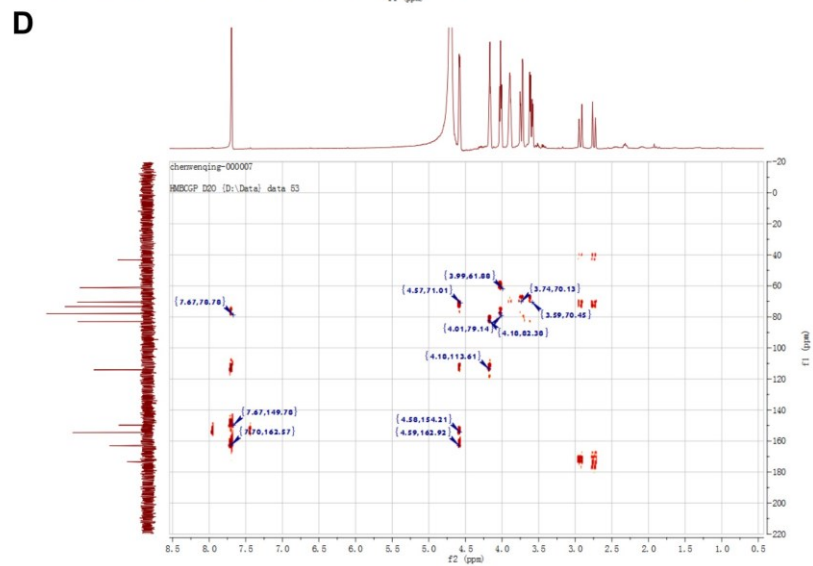
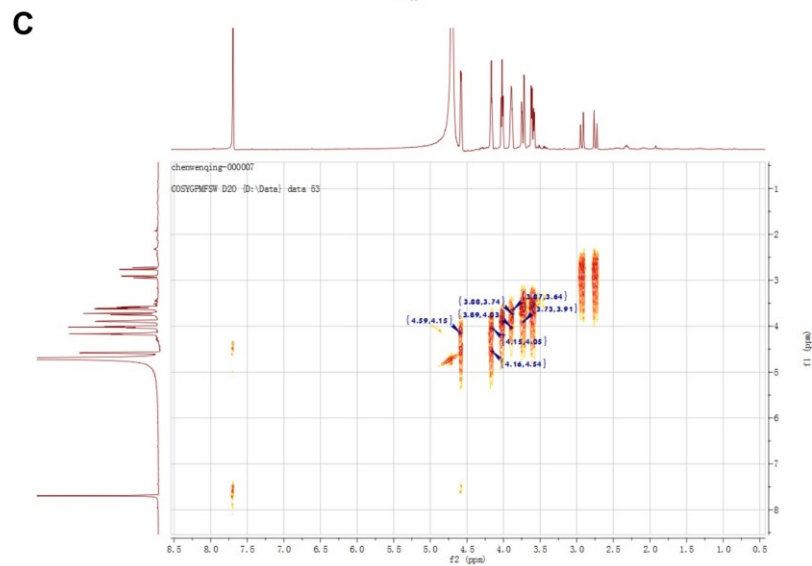
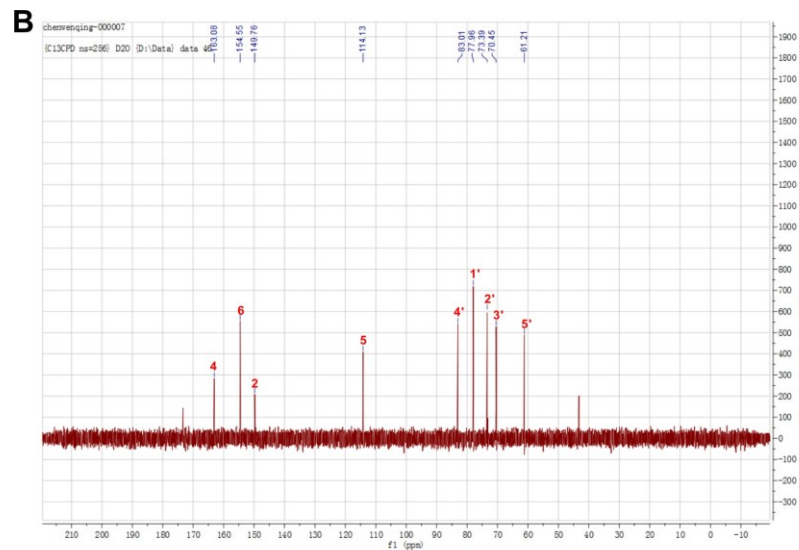
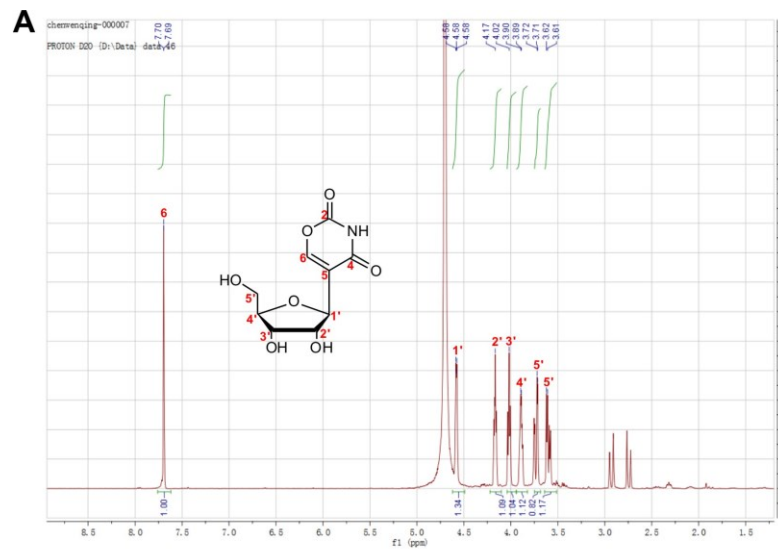


Figure S2. NMR data of MIN, Related to Figure 2.

(A) ^1H NMR spectrum of MIN. (B) ^{13}C NMR spectrum of MIN. (C) ^1H - ^1H COSY NMR spectrum of MIN. (D) HMBC NMR spectrum of MIN. NMR (400 MHz, D_2O).

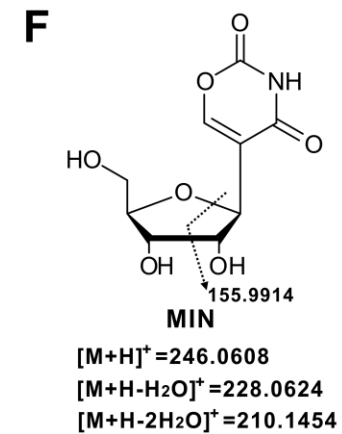
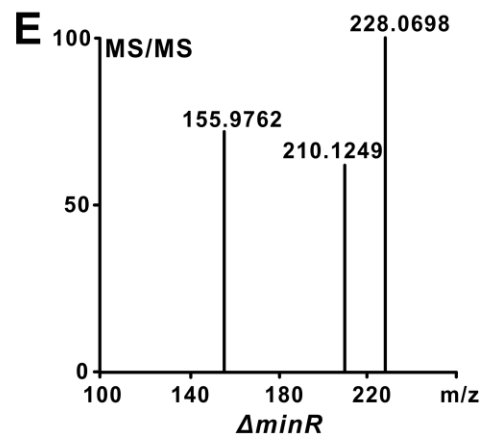
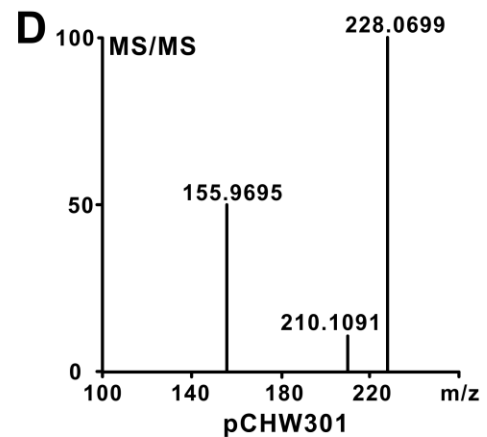
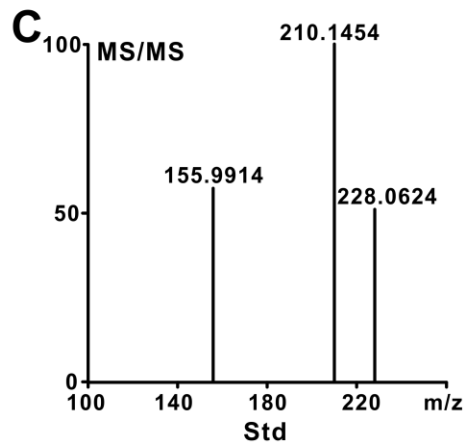
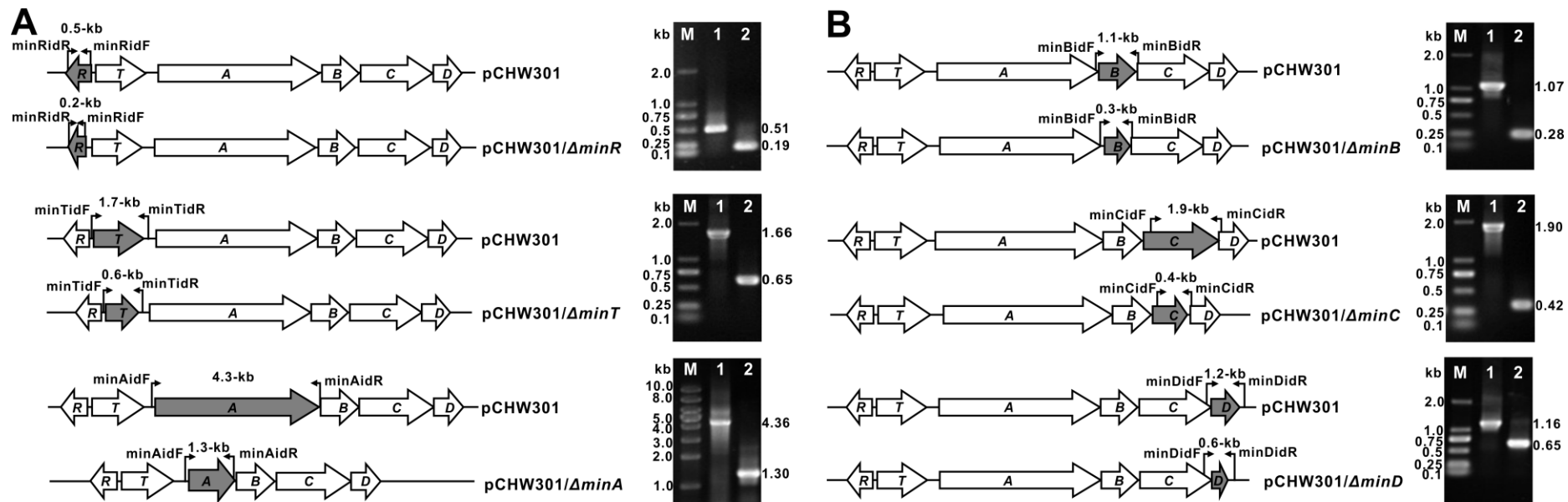


Figure S3. In frame deletion of *min* genes and metabolites analysis of related *S. coelicolor* recombinants, Related to Figure 2.

(A) In frame deletion of the target gene in pCHW301 by *in vitro* CRISPR/Cas9 Editing technology. Left column, schematic illustration for the targeted mutation of the *min* genes ($\Delta minR$, $\Delta minT$, and $\Delta minA$). Right column, PCR identification of the targeted mutation of the *min* genes (which corresponds to that in left column). M, 1 kb ladder (ComWin Biotech) or DM2000 ladder (ComWin Biotech); 1, PCR product using pCHW301 as template; 2, PCR product using individual pCHW301 variant as template.

(B) In-frame deletion of the target gene in pCHW301 by *in vitro* CRISPR/Cas9 Editing technology. Left column, schematic illustration for the targeted mutation of the *min* genes ($\Delta minB$, $\Delta minC$, and $\Delta minD$). Right column, PCR identification of the targeted mutation of the *min* genes (which corresponds to that in left column). M, 1 kb ladder (ComWin Biotech) or DM2000 ladder (ComWin Biotech); 1, PCR product using pCHW301 as template; 2, PCR product using individual pCHW301 variant as template.

(C) HRMS/MS analysis of the authentic MIN standard. (D) HRMS/MS analysis of the product (MIN) produced by *S. coelicolor* M1154::pCHW301. (E) HRMS/MS analysis of the target metabolite (MIN) produced by *S. coelicolor* M1154::pCHW301 $\Delta minR$. (F) Fragmentation pattern of the authentic MIN standard.

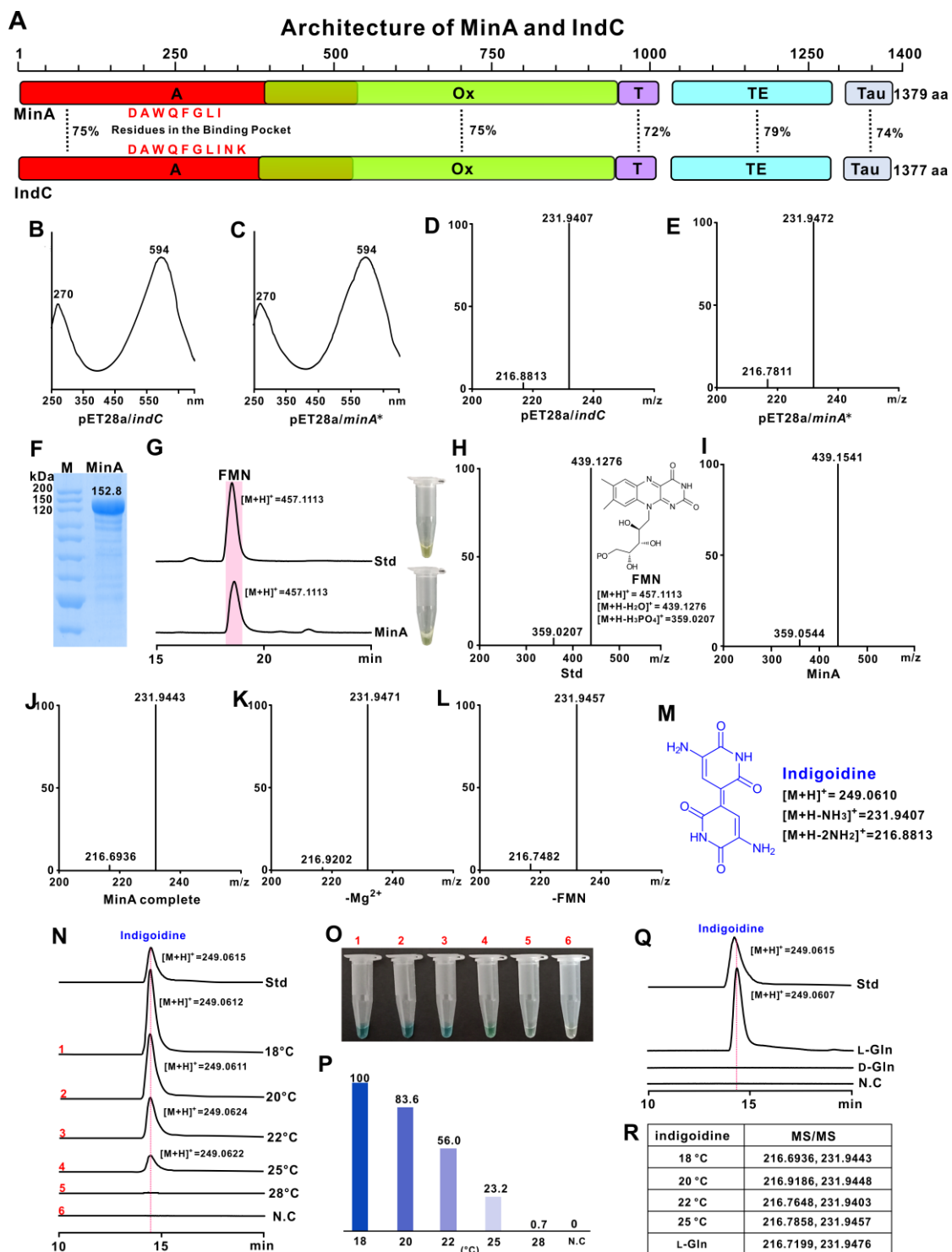


Figure S4. Architectural analysis and biochemical characterization of MinA as an NRPS enzyme governing indigoidine biosynthesis, Related to Figure 3.

(A) The domain-architecture of MinA and IndC. As indicated, both MinA and IndC consist of A domain (adenylation), Ox domain (oxidoreductase), T domain (thiolation), TE domain (thioesterase), and Tau domain (tautomerase), and related homologies corresponding to individual domains have also been indicated. (B-C) UV spectrum of

indigoidine produced by *E. coli* BAP1 containing pET28a/*indC* (positive control) and pET28a/*minA*^{*}, respectively. (D-E) LC-HRMS/MS analysis of indigoidine produced by *E. coli* BAP1 containing pET28a/*indC* (positive control) and pET28a/*minA*^{*}, respectively. (F) SDS-PAGE analysis of MinA (152.8 kDa). (G) Characterization of the cofactor bound in MinA as FMN. Std, the authentic FMN standard; MinA, the cofactor FMN obtained from MinA; the color of the samples is consistent with the result of HPLC analysis. (H-I) LC-HRMS/MS analysis of the authentic FMN standard and that purified from MinA. (J-L) LC-HRMS/MS analysis of indigoidine in MinA reaction using L-Gln as substrate. MinA complete, complete MinA reaction; -Mg²⁺, MinA reaction without Mg²⁺ added; -FMN, MinA reaction without FMN added. (M) Fragmentation pattern of indigoidine produced by *E. coli* BAP1 containing pET28a/*indC*. (N) HPLC analysis of MinA reaction under different temperatures. Std, indigoidine produced by *E. coli* BAP1 containing pET28a/*minA*^{*}; 18°C, 20°C, 22°C, 25°C, and 28°C indicate MinA reaction conducted at 18°C, 20°C, 22°C, 25°C, and 28°C, respectively; N.C, the reaction without MinA added as negative control. (O) The color of indigoidine isolated from MinA reaction mixture. 1-5, MinA reaction conducted at 18°C, 20°C, 22°C, 25°C, and 28°C, respectively; 6, the reaction without MinA added as negative control. (P) Relative productivity of indigoidine produced by MinA reaction at different temperatures. (Q) HPLC analysis of MinA reaction using different substrates. Std, the authentic indigoidine standard; L-Gln, MinA reaction with L-Gln as substrate; D-Gln, MinA reaction with D-Gln as substrate; N.C, the reaction without MinA added as negative control. (R) LC-HRMS/MS of indigoidine. 18°C, 20°C, 22°C, and 25°C represent MinA reaction conducted at 18°C, 20°C, 22°C, and 25°C, respectively; L-Gln, MinA reaction with L-Gln as substrate.

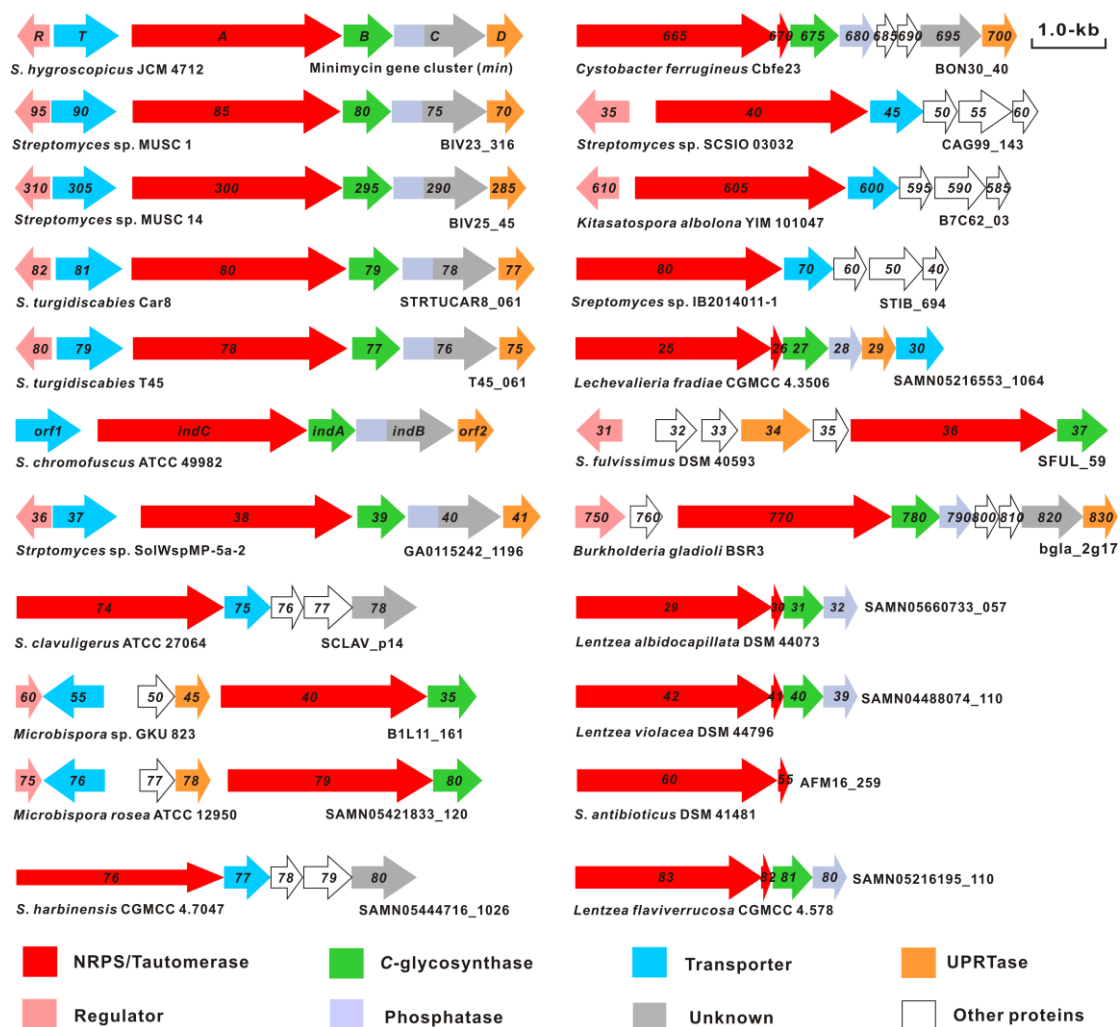


Figure S5. MinA-directed genome mining of the gene clusters for potential C-nucleoside compounds, Related to Figure 5.

The potential gene clusters of the C-nucleoside compounds were obtained using MinA as query sequence.

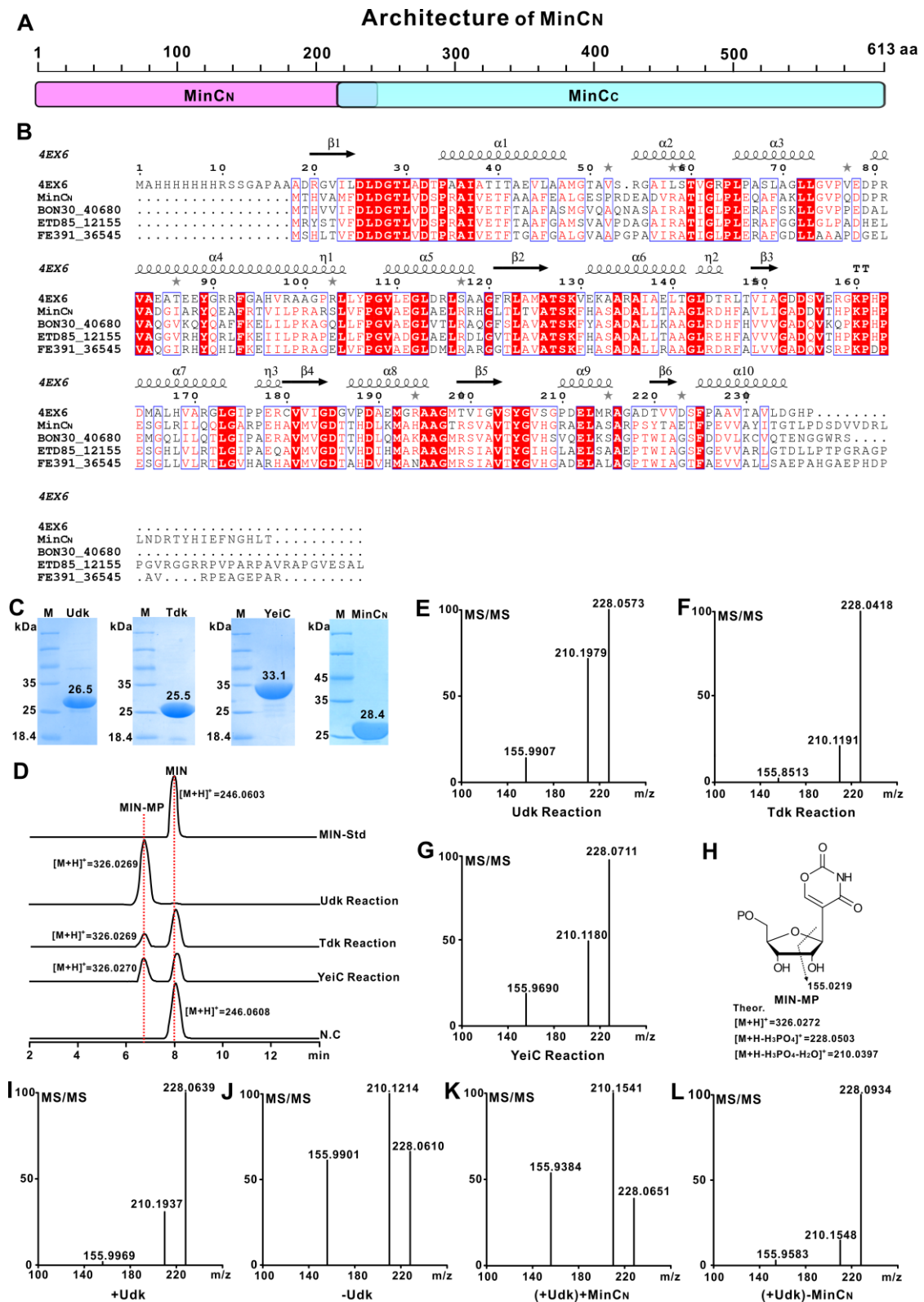


Figure S6. Functional analysis of MinC_N as phosphatase governing the final dephosphorylation step, Related to Figure 4.

(A) The domain-architecture of MinC. As indicated above, MinC comprises a MinC_N domain (HAD phosphatase domain shown in purple) and a MinC_C domain (DUF4243

domain shown in blue). (B) Bioinformatic analysis of MinC_N with its homologs. Secondary structure of 4EX6_A is displayed on the top. 4EX6_A (PDB: 4EX6_A) from *Streptomyces turgidiscabies* Car8; ETD85_12155 (GenBank: TMR35971) from *Nonomuraea zaeae*; FE391_36545 (GenBank: TLF58285) from *Nonomuraea* sp. KC401. (C) SDS-PAGE analysis of the proteins Udk (26.5 kDa), Tdk (25.5 kDa), YeiC (33.1 kDa), and MinC_N (28.4 kDa). (D) LC-HRMS analysis of reaction-mixtures of Udk (GenBank: QBJ70019.1, from *Bacillus subtilis* CGMCC 1.338), Tdk (GenBank: AL939125.1, from *S. coelicolor* M1154), and YeiC (GenBank: AL939111.1, from *S. coelicolor* M1154), using MIN as substrate. MIN-Std, the authentic MIN standard; Udk Reaction, the reaction catalyzed by Udk; Tdk Reaction, the reaction catalyzed by Tdk; YeiC Reaction, the reaction catalyzed by YeiC; N.C, the reaction without enzyme added as negative control. (E-G) LC-HRMS/MS analysis of target product (MIN-MP) produced by Udk reaction, Tdk reaction, and YeiC reaction, respectively. (H) Fragmentation pattern of the MIN-MP standard. (I) LC-HRMS/MS analysis of target product (MIN-MP) produced by Udk reaction. (J) LC-HRMS/MS analysis of MIN without Udk added. (K) LC-HRMS/MS analysis of MIN produced by MinC_N reaction, using the substrate MIN-MP supplied by Udk reaction, but Udk was removed before addition of MinC_N. (L) LC-HRMS/MS analysis of MIN-MP produced by Udk reaction, and MinC_N was not added after removal of Udk.

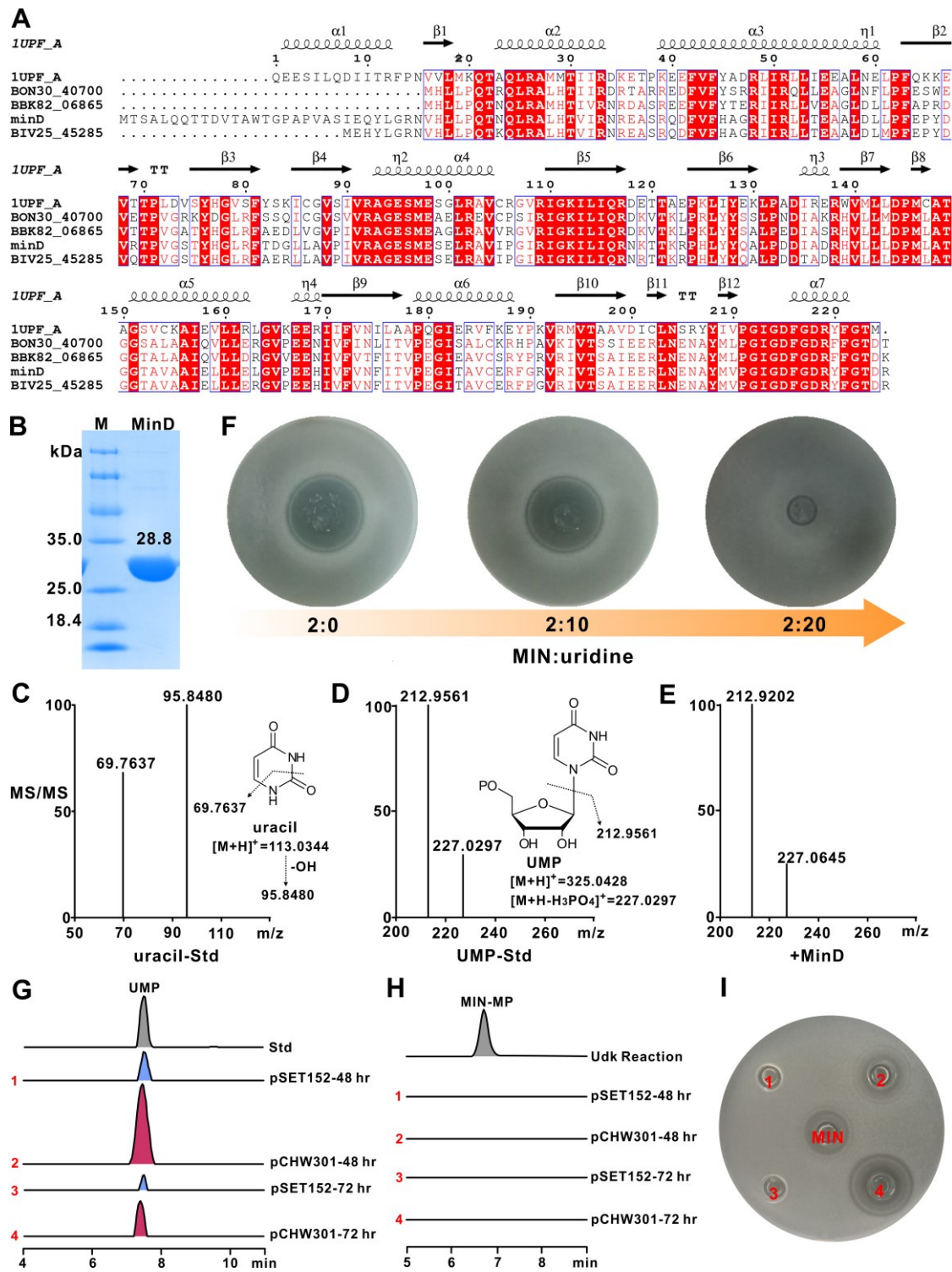


Figure S7. Functional characterization of MinD as the key safe-guard enzyme, Related to Figure 4 and 6.

(A) Bioinformatic analysis of MinD with its homologs. Secondary structure of 1UPF_A is shown on the top. 1UPF_A (PDB: 1UPF_A) from *Toxoplasma gondii*; BIV25_45285 (GenBank: OIJ84979) from *Streptomyces* sp. MUSC 14; BBK82_06865 (GenBank: ANZ42539) from *Lentzea guizhouensis*; BON30_40700 (GenBank: OJH35070) from

Cystobacter ferrugineus. (B) SDS-PAGE analysis of MinD (28.8 kDa). (C) LC-HRMS/MS analysis and fragmentation pattern of the authentic uracil standard. (D) LC-HRMS/MS analysis and fragmentation pattern of the UMP standard. (E) LC-HRMS/MS analysis of target product (UMP) produced by MinD reaction. (F) Bioassay of MIN mixed with uridine. The ratios of MIN and uridine are 2:0 (2 µg:0 µg), 2:10 (2 µg:10 µg), and 2:20 (2 µg:20 µg), respectively. *Bacillus subtilis* CGMCC 1.338 was used as indicator strain. (G) LC-HRMS analysis of the *in vivo* UMP concentrations for related strains. Std, the authentic standard of UMP; “pSET152-48hr” and “pSET152-72 hr” indicate the relative abundance of UMP concentrations (*in vivo*) of *S. coelicolor* M1154::pSET152 grown at 48 hr and 72 hr, respectively; Likewise, “pCHW301-48 hr” as well as “pCHW301-72 hr” indicates the relative abundance of UMP concentrations (*in vivo*) of *S. coelicolor* M1154::pCHW301 correspondingly grown at 48 hr and 72 hr. (H) LC-HRMS analysis of the *in vivo* MIN-MP concentrations for related strains. Udk Reaction, the Udk catalyzed reaction to form MIN-MP as positive control; “pSET152-48 hr” and “pSET152-72 hr” indicate the *in vivo* MIN-MP concentrations of *S. coelicolor* M1154::pSET152 in 48 hr and 72 hr, respectively; Similarly, “pCHW301-48 hr” and “pCHW301-72 hr” individually represent the *in vivo* MIN-MP concentrations of *S. coelicolor* M1154::pCHW301 in 48 hr and 72 hr. (I) Bioassay of MIN produced by related strains. MIN, the authentic standard of MIN; 1 and 3, the fermentation broth of *S. coelicolor* M1154::pSET152 grown at 48 hr and 72 hr, respectively; 2 and 4, the fermentation broth of *S. coelicolor* M1154::pCHW301 correspondingly grown at 48 hr and 72 hr.

2. Supplementary Tables

Table S1. Strains and plasmids used in this study, Related to Figure 2-4, and 6.

Strain/Plasmid	Relevant characteristics*	Reference or source
Strain		
<i>S. hygroscopicus</i> JCM 4712	Wild-type of MIN producer	JCM
<i>S. coelicolor</i> M1154	<i>S. coelicolor</i> A3(2) derivative	(Gomez-Esc ribano and Bibb, 2014)
<i>Bacillus subtilis</i> CGMCC 1.338	Indicator strain for MIN bioassay	CGMCC
M1154::pCHW301	<i>S. coelicolor</i> M1154 containing pCHW301	This study
M1154::pSET152	<i>S. coelicolor</i> M1154 containing pSET152	This study
M1154::pCHW301/ Δ minA	<i>S. coelicolor</i> M1154 containing pCHW301/ Δ minA	This study
M1154::pCHW301/ Δ minB	<i>S. coelicolor</i> M1154 containing pCHW301/ Δ minB	This study
M1154::pCHW301/ Δ minC	<i>S. coelicolor</i> M1154 containing pCHW301/ Δ minC	This study
M1154::pCHW301/ Δ minD	<i>S. coelicolor</i> M1154 containing pCHW301/ Δ minD	This study
M1154::pCHW301/ Δ minT	<i>S. coelicolor</i> M1154 containing pCHW301/ Δ minT	This study
M1154::pCHW301/ Δ minR	<i>S. coelicolor</i> M1154 containing pCHW301/ Δ minR	This study
M1154::pIB139	<i>S. coelicolor</i> M1154 containing pIB139	This study
M1154::pIB139/ <i>minD</i>	<i>S. coelicolor</i> M1154 containing pIB139/ <i>minD</i>	This study
M1154::pIB139/ <i>minT</i>	<i>S. coelicolor</i> M1154 containing pIB139/ <i>minT</i>	This study
M1154::pIB139/ <i>minC_N</i>	<i>S. coelicolor</i> M1154 containing pIB139/ <i>minC_N</i>	This study
M1154::pIB139/ <i>minDT</i>	<i>S. coelicolor</i> M1154 containing pIB139/ <i>minDT</i>	This study
M1154::pIB139/ <i>minDC_N</i>	<i>S. coelicolor</i> M1154 containing pIB139/ <i>minDC_N</i>	This study
M1154::pIB139/ <i>minTC_N</i>	<i>S. coelicolor</i> M1154 containing pIB139/ <i>minTC_N</i>	This study
M1154::pIB139/ <i>minDTC_N</i>	<i>S. coelicolor</i> M1154 containing pIB139/ <i>minDTC_N</i>	This study
<i>E. coli</i> DH10B	F ⁻ , <i>mcrA</i> , Δ (<i>mrr-hsdRMS-mcrBC</i>), ϕ 80d, <i>lacZ</i> Δ M15, Δ <i>lacX74</i> , <i>deoR</i> , <i>recA1</i> , <i>endA1</i> , <i>araD139</i> , Δ (<i>ara, leu</i>)7697, <i>galU</i> , <i>galK</i> , λ ⁻ , <i>rpsL</i> , <i>nupG</i>	Gibco-BRL
<i>E. coli</i> BAP1	BL21(DE3) Δ <i>prpRBCD</i> ::T7prom- <i>sfp</i> , T7prom- <i>prpE</i>	Kerafast
<i>E. coli</i> Rosetta(DE3)/pLysS	F ⁻ , <i>ompT</i> , <i>hsdS_B</i> (<i>r_B⁻m_B⁻</i>), <i>gal dcm</i> λ (DE3) pLysS(CmI ^R)	Novagen
<i>E. coli</i> ET12567(pUZ8002)	ET12567 with plasmid pUZ8002(Kan ^R)	(Kieser et al., 2000)
Plasmid		
pEASY-Blunt	pUC ori, <i>lacZ</i> , f1 ori, Kan, Amp	TransGen Biotech
pSET152	<i>aac(3)IV</i> , <i>lacZ</i> , <i>attP</i> (Φ C31), <i>oriT</i>	(Bierman et al., 1992)
pET28a	Kan, <i>rep</i> ^{pMB1} , T7 promoter	Novagen
pIB139	<i>int</i> , <i>attP</i> , <i>aac(3)IV</i> , <i>PerME</i> *	(Vecchio et

pJTU968	pRSETb derivative with T7 promoter replaced by <i>Perme*</i>	(Zhou et al., 2011)
pET28a/ <i>minA*</i>	pET28a derivative carrying a NdeI-EcoRI fragment containing <i>minA*</i>	This study
pET28a/ <i>indC</i>	pET28a derivative carrying a NdeI-EcoRI fragment containing <i>indC</i>	This study
pET28a/ <i>minC_N</i>	pET28a derivative carrying a NdeI-EcoRI fragment containing <i>minC_N</i>	This study
pET28a/ <i>udk</i>	pET28a derivative carrying a NdeI-EcoRI fragment containing <i>udk</i>	This study
pET28a/ <i>tdk</i>	pET28a derivative carrying a NdeI-EcoRI fragment containing <i>tdk</i>	This study
pET28a/ <i>yeiC</i>	pET28a derivative carrying a NdeI-EcoRI fragment containing <i>yeiC</i>	This study
pET28a/ <i>minD</i>	pET28a derivative carrying a NdeI-EcoRI fragment containing <i>minD</i>	This study
pIB139/ <i>minD</i>	pIB139 derivative carrying a NdeI-EcoRI fragment containing <i>minD</i>	This study
pIB139/ <i>minT</i>	pIB139 derivative carrying a NdeI-EcoRI fragment containing <i>minT</i>	This study
pIB139/ <i>minC_N</i>	pIB139 derivative carrying a NdeI-EcoRI fragment containing <i>minC_N</i>	This study
pIB139/ <i>minDT</i>	pIB139 derivative carrying a NdeI-EcoRI fragment containing <i>minD</i> and <i>minT</i>	This study
pIB139/ <i>minDC_N</i>	pIB139 derivative carrying a NdeI-EcoRI fragment containing <i>minD</i> and <i>minC_N</i>	This study
pIB139/ <i>minTC_N</i>	pIB139 derivative carrying a NdeI-EcoRI fragment containing <i>minT</i> and <i>minC_N</i>	This study
pIB139/ <i>minDTC_N</i>	pIB139 derivative carrying a NdeI-EcoRI fragment containing <i>minD</i> , <i>minT</i> and <i>minC_N</i>	This study
pCHW301	pSET152 derivative carrying a XbaI-EcoRI fragment containing whole <i>min</i> gene cluster	This study
pCHW301/ Δ <i>minA</i>	pCHW301 derivative with <i>minA</i> in-frame deleted	This study
pCHW301/ Δ <i>minB</i>	pCHW301 derivative with <i>minB</i> in-frame deleted	This study
pCHW301/ Δ <i>minC</i>	pCHW301 derivative with <i>minC</i> in-frame deleted	This study
pCHW301/ Δ <i>minD</i>	pCHW301 derivative with <i>minD</i> in-frame deleted	This study
pCHW301/ Δ <i>minT</i>	pCHW301 derivative with <i>minT</i> in-frame deleted	This study
pCHW301/ Δ <i>minR</i>	pCHW301 derivative with <i>minR</i> in-frame deleted	This study

Table S2. Primers used in this study, Related to Figure 2-4, and 6.

Primers	Sequence (5'--3')
Piece1-F	GACTAGTTCAGTCGTCAACCTGGGT
Piece1-R	TGGAGAGGAACCGTTCCTTC
Piece2-F	GCAGCAAGCCGACCTCGCAC
Piece2-R	GGAATTCGGCTGCCGCTCCTGAAGCAC
min id-F	ACCGCCAACGGGAAGATC
min id-R	GAACGAATAGCCGCACAGG
sgRNA/A	AAAAGCACCGACTCGGTGCCACTTTTTCAAGTTGATAACGGACTAGCCTTATTTAACTT GCTATTTCTAGCTCTAAAAC
minA-sgL	GATCACTAATACGACTCACTATAGTGATGGTGCGGACTCCGGCGTTTTAGAGCTAGAAA
minA-sgR	GATCACTAATACGACTCACTATAGCCGGGCGGACTTCGCCGACGTTTTAGAGCTAGAAA
minAidF	AGAGGGCGTGAATTTGCT
minAidR	CGGCGGTCAGTAGTTGG
minB-sgL	GATCACTAATACGACTCACTATAGGCTCGCCGCCACCGTTTTAGAGCTAGAAA
minB-sgR	GATCACTAATACGACTCACTATAGTGCCGCGTTGTCCGGGTAGTTTTAGAGCTAGAAA
minBidF	CGCAAGACGCCAACTAC
minBidR	CCCGTCCAGGTCGAACAT
minC-sgL	GATCACTAATACGACTCACTATAGCTGGGCCCGAATGGGACGTTTTAGAGCTAGAAA
minC-sgR	GATCACTAATACGACTCACTATAGCGACGCGGGGGTCTCCTGGTTTTAGAGCTAGAAA
minCidF	CCACTTCGCCGTGCTGA
minCidR	GTCGAGGGCGCCTCGGTCA
minD-sgL	GATCACTAATACGACTCACTATAGCGCGCAGCTGGTTCGTCTGGTTTTAGAGCTAGAAA
minD-sgR	GATCACTAATACGACTCACTATAGCGAGCGCTTCGGCCGGGTGGTTTTAGAGCTAGAAA
minDidF	TGGGCGTGCTGTTCTCC
minDidR	CGGCAGCCTTGTTTCAGG
minT-sgL	GATCACTAATACGACTCACTATAGAGCGGTCCGGGTACGCCGTTTTAGAGCTAGAAA
minT-sgR	GATCACTAATACGACTCACTATAGCGACAGCGCCACCGTCGTCGTTTTAGAGCTAGAAA
minTidF	CACCTGGTTTTGACAGTGGTT
minTidR	CGCAGTAGCGGGCATT
minR-sgL	GATCACTAATACGACTCACTATAGTGGGGATGCGCGAGCCACGTTTTAGAGCTAGAAA
minR-sgR	GATCACTAATACGACTCACTATAGGGACAAGGCCTGGTCGGACGTTTTAGAGCTAGAAA
minRidF	GCCTCCGACGGCAGAT
minRidR	GGGGCGTAGTTCCTCACC
indCexF	GTCCATATGAGCGTAGAGACCATC
indCexR	CCGCTCGAGTCAGTAGTTGGGCGTCTT
minC _N exF	GTCCATGTGACACACGTGGCGATG
minC _N exR	GGAATTCGGTCAGGTGACCGTTGAA
tdkexF	GTCCATATGCCGAGCTGGTGTT
tdkexR	GGAATTCTCACGTGGCGGTGACCGG
yeiCexF	GTCCATATGTACGACTACGACCTG
yeiCexR	GGAATTCTCACAGCGCCCCGGCCCC
minTexF	GTCCATATGATCTGCCGTGTGACG
minTexR	GGAATTCTCAGCCGATCTGGCGGTT

minDTidF	ATCGTGACCTCCGCAATC
minDTidR	GGCTGTGACGGACCTCTT
minDC _N idF	ATTCAGCGGAACAAAACG
minDC _N idR	GCGAAGGTCTCGACGATC
minTC _N idF	GTTGTTCTCCGGCACCTC
minTC _N idR	GCGAAGGTCTCGACGATC

Table S3. NMR data of minimycin in D₂O, 400MHz, Related to Figure 1.

NO.	¹ H (δ,multi)	¹³ C (δ)
2		149.76
4		163.08
5		114.13
6	7.70(S,1H)	154.55
1'	4.58(S,1H)	77.96
2'	4.17(S,1H)	73.39
3'	4.02(S,1H)	70.45
4'	3.90(S,1H)	83.01
5'	3.72(S,1H),3.62(S,1H)	61.21

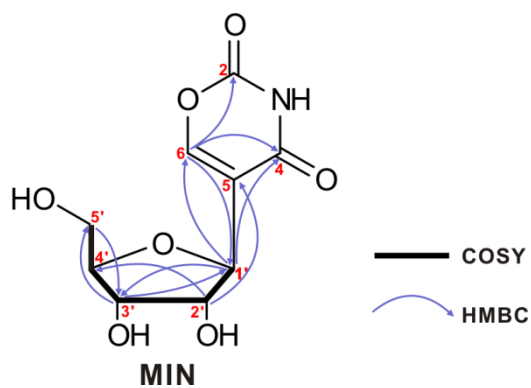


Table S4. Validation of the pCHW301 variants by sequencing analysis, Related to Figure 2.

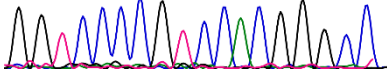
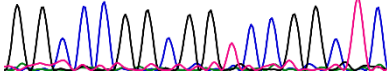
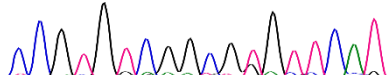
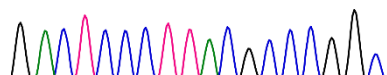
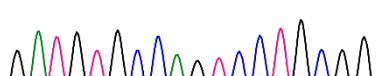
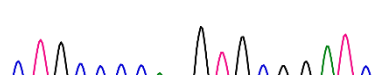
Plasmid	Determined sequence	Theoretical sequence
pCHW301/ Δ <i>minR</i>	 GGT CCC CGT CCA CGG GCC	GGT CCC CGT CCA CGG GCC
pCHW301/ Δ <i>minT</i>	 GGC CCG GCG GTC CGG CTC	GGC CCG GCG GTC CGG CTC
pCHW301/ Δ <i>minA</i>	 CCG TGT CGG CGT GTT CAT	CCG TGT CGG CGT GTT CAT
pCHW301/ Δ <i>minB</i>	 GAC TCC CTT ACG CCC GGC	GAC TCC CTT ACG CCC GGC
pCHW301/ Δ <i>minC</i>	 GAT GTG CCA GTC CTG CGG	GAT GTG CCA GTC CTG CGG
pCHW301/ Δ <i>minD</i>	 CTG CCC CAG GTG CGG ATC	CTG CCC CAG GTG CGG ATC

Table S5. Optimized sequence for *minA*, Related to Figure 3.

ATGAGCCCTCACGTTATCCCCACACCCAGCGCGGTGACGTTTGTAAACCGCACTGCTGGCCGAGCAG
GCGAGTGCAGCACCTCATAGAACCGCAGTTGTTACGAAGACCAGAGCCTGACGTTTGCACAGCTGTT
AGATCATTCCAGATTATTAGGTGCACGTTTACGGCGTGCCGGTGTACCCGTGGTAGTAGAGTTGGTG
TTTTATGGAGCCGAGCCTGGAATTAATGACCAATGTTGGGGTATTCTGTGGGCAGGTGGTAGCTAT
GTTCCGCTGAGCCCTGAATATCCGGAGGAACGTATTGCATATATGATGGCAGATGCAGGAGTTGAAGT
TGTTCTGACGCAGGAATTTCTGCGTTCACGTTTACAGGAGCTGTCACCGGCAGGTGTTCTGACCATTAC
CAGCGATGAGGTTTTTATTCTGTTGAATCAGCGGATGAGGAGATTAGTAGTCCGGGCTTAGAGTCTT
GTCAGGCCGCACGTCCAGAAGATTTAGCATACGTTATTTATAAAGCGGCAGCACGGGGAAGCCGAA
AGGTGTTATGATTGAACATAGAAGCATCGTTAGCCAAATGCGGTGGCTGACCGAAGCATGTGGTATAG
ATGGGGTTCGTACCATTCTGCAGAAAACCCCGCTGAGCTTGTATGCCGCACAGTGGGAAATTTAGCA
CCGGCATGCGGTAGCACAGTTGTAATGGGTGCACCGGGTATTTATCGTGATCCGGAAGCAATCGTTGC
CACCATTAGAGACATGGTGTACAACCTTACAGTGTGTTCCGACCTTACTTCAAGCCCTGCTGGACAC
CGAAACCTTAGCAGGTTGTGGTCTTTACGTCAAGTGTCTTCTGGTGGTGAAGCGTTATCACGTAGTCT
GGCCGCCAGTTTTCTGATACCATGCCGGATTGTAGTTTAGTTAATCTGTATGGCCCGACCGAGTGTAC
AATTAATGCAAGCGCATTGTTGTTGATCGGACCGCTGTTGAAGATGGTCCGAGAGTTATGCCTATTGG
TACACCTGTTAGTGGTACCACCTTTCATGTTCTGGATAGCGCAGGTCGGGAGGCCACAGTAGGTGAAG
TTGGTGAAGTGCACATTGGGGGATTACAGTTGCACGTGGGTATCTGGGGCGCCCTGATTTAACAGCA
GAACGTTTTGTTGAGGATACATTTAGCAGCGTTCGGGTGCACGGCTGTATCGTACAGGTGATTTAGCA
CATTTAATGCGGATGGTACAGTTCAATTTGTTGGTCTGACCGATAATCAGGTTAACTGCGTGGGTAT
CGTGTGAATTAGATGAAATTAGACAGGCCATTGAAACGCATGATTGGGTTCGTAGCAGTGCAGTTCT
GTTACGGGATGATGAAGCTACCGGGTCCAAAATCTGGTTGCATTTGTTGAGCTGAATCCCAAGGAGG
CAGCATTAAATGGATCAGGGTAATCATGGTGCACATCACCAGAGTAAACGTAGTAGACTGCAGGTTCTG
GCCAGCTGAGCCATGCAGGTTGTCGTGATGCAGCAGATCTGGCAGGGCGTTCGGTGCACAGCATTACC
GGGTGCAGAAGCAACCCCGAACAGAGAGCAAGAGCATTGTCACGTAACCTATCGTTTTTATGAAG
GGGGTCAGGTTAGTCGGGAAGATATTCTGCGTTTACTGGCACCGCCGGTAGACCTGGAGTTCACCT
AGAAATCCGGGTAGCTTAAATCGTGCAGAACTGGGTGGTATTCTGCGGAATTTGGCCAGTATTTAAG
CGATCAGCGTCTGTTACCTAAATATGCATACGCTAGTCCGGGGAGTCTTTATGCAACCCAGTTATATT
AGAACTTGATGGTATTGGGGGGATTGGTCCGGGTTATATTATTATCACCTTTACATCACCCTTAGT
GCTGATTGGCCGACCCCGAGACAGTCTGGTCTAGAGCATCCATTCTGCTGGGTAAACACAGTG
CAATTGAACCTGTTTATCGTAACAATATTCTGAGGTTCTTGAATTTGAAGCAGGGCACATGGTTGGTT
TATTCGAAGAGTTTTACCGGATTACGTTTAGGTATTGCAGCAGAATATCGGCCGGCAGTTCTGCATC
GTCTGGAAGGTGCGGAAGAAGATCACTATTTAGGTACCATTGATCTGGTCCCGTATGATGCAAATGAA
AGCGCCGATGAGCTGGACATTTATGTGCAAGCACACGCAGGACGTGTTGATGGTCTGCGTGCAGGTC
AGTATCGTTATGCCGATGGCAGCTTAGTTCGTATTTGCGATGATTTAGTTCTGAAGAAACATGTTATCG
CGATTAATCAGCGTGTATGAGCGTGCGGGTCTGGGTATTAGTTTAGTTGCGACCGGTCCGGATTCTAT
GGCGTCAATTCTGGATTAGGGCGCAAGTTACAGCGTTTACAGATGAACGGGGCTGAATTTAGGTTTT
ATGAGTAGTGGTTACAGCAGCAAGAGCGGTAATGACTTACCGCGCGGAAACGTTTAAATCGTATTCT
GACAGATTGTGGGTTACCTACGGGTCCGTCGATTTTTTTGTTGGTGGGCGGGTTAGCGATGAACAGT
TACGTGGTGAAGATATGAAAGAAGATGTTGTTACATGCAGGGTCCGGCAGAAGTATTAAGGAGGA
TTAGCAGGTCTGCTGCCGCTTATATGCTGCCTAATAGAATTGTTGTGCTGGATCGTCTGCCGCTGAC
CGCAAATGGGAAAATAGACAGCAAAGCTTTGAAGCCAGCCAGCAGGCGGATTTAGCATTAGCAGCA
AGAACCTTATAGCACCGCGGACCCGTGTTGAACGGAGAGTACGTGATCTGTGGCAGACAGTGTGA
AACAGGAACAGATAAGCGTGCGGGATGATTTTTTGTAGCTGGGGGTAATAGCCTGCTGGCGGTTGC
ATTAGTTAATCGTATGAATAAAGCATTTCGAGGGTACGGTTCGCTGCAAGTGTATTTGATGCCCGAC
CGTTGAAAAGCTGGCCGCAAGACTTGTGAGCAACCTTCTGGTCCGTTAACCCGCTGTTTCCGCTGCA
GCCTGAGGGTACAGGTACCCCTATTCTGTTGGCCGGTTTAGGTGGTTATCCGATGAATCTGAGAC
CGTTAGCAGCAGCACTTGGTAAAGATCGTCCGGTTCATGGTATTAGGCACATGGGATTAATCGTGGC
GAAGATCCGATGCGACCGTTCGTGAAATGGCGACCGCGGATGTTGAAGCAATTCGTAGTGCACAGCC
GGAAGGGCCTTATTTTTATGTGGCTATAGCTTTGGGGCACGCGTTGCATTTGAAGCCGCCAGACAGC
TGGAACAGGCGGGTCAACGTGTTGAGCATTATTTTTAATTGCACCGGGTATGCCGCTGCTGCGTGAG
GAAGATACCGCAGGTCCGACCGGTAGAGCAGATTTTGCAGATCGGGCATTGTGGCACTGCTGCATAG
TGTTTTGCCGGTACCCTGAGCGGTCCGCAGTTAGATGATTGTTAAGAACAGTTACCGATGAAGATAG

CTTTGTGGATTTTGTACCAGCCGTTTTCCGGGTTTAGGTACCGAACTGGTTCAGGCAGTTACCGGTAT
TGTTAAACGTACCTATAGCCCGACCTACGAATTTATGAACACTGACCGGGCGTCGTCTGAACGCACCTGT
AAACTGGTTAAAGCAAATGACGATAATTATTCATTCATCGAACACCAGGATGCATTTTCAGTTAGACC
TCCGAGCGTGCATCAACTGCCTAGCGGTCATTATGAACTGCTGCGTGAACCACATGTTACCGAATTAGC
AGCACTGGTCAACGATCGCCTGCGCACAGCAGCAGGTAGCCCTTTCCGGGTCAAGTGTCTATTATCTCG
TGTTATTTACAGGAGGCCGGTGTCCGCATATTAATATTAACATTTCCAGTTGCCCTGAGCGAAGC
ACAGGAAAAAGAACTGCTGGCAGCCTTAACAAGCGCAGTCTCCAATGCATTTGGTTGTAAGAAGATG
TTGTGAGTATTGCCATAGAACCGGTCGAGCAAGAAGCATGGCACGAACGGGTGTATGAACCGGAAAT
CGTACGTCGCCAGGATCTGCTGCGCAAACCCCAAATTATTA

Table S6. Optimized sequence for *udk*, Related to Figure 4.

ATGGGCACCAATAAACCGGTTGTTATTGGTATTGCCGGTGGTAGCGGTAGTGGTAAAACCAGCGTTAC
CAAAGCAATCTTCGATCATTTTAAAGCCATAGCATTCTGATCCTGGAACAGGATTACTATAAGGAT
CAGAGCCATCTGCCGATGGAAGAACGTCTGAAAACCAATTATGATCATCCGCTGCCCTTTGATAACGAT
CTGCTGATTGAACATCTGCAGCAACTGCTGGCATATAAACAGGTTGATAAACCCGTGTATGATTATACC
CTGCATACCCGTAGCGAAGAAATTATCCGGTTGAACCGAAAGATGTGATTATTCTGGAAGGTATCCTG
ATACTGGAAGATCCGCGTCTGTGTGAACTGATGGATATTAACCTGTTTGTGATACCGATGCCGATCTG
CGTATTCTGCGTCGTATGCAGCGTGATATTAAGAACGTGGTCGTACCATGGATAGCGTGATTGATCAG
TATGTTAATGTTGTTTCGTCGGATGCACAACCAGTTTATCGAACCGAGCAAAAAATTCGCCGATATCATT
TCCCGAAGGTGGTCAGAATCATGTTGCCATTGATATTATGGTGACCAAAATTGCCACCATCCTTGAAC
AGAAAGTGAACCTGTAA

3. Transparent Methods

General methods

General methods employed in this work were according to the standard protocols of Green *et al.* (Green and Sambrook, 2002) or Kieser *et al.* (Kieser et al., 2000).

Enzymes, chemicals, and reagents

All of the enzymes used in this study were purchased from New England Biolabs. The chemicals and reagents were the products of Sigma-Aldrich, Thermo Scientific, OMEGA, or J&K Scientific.

Sequencing analysis of *S. hygrosopicus* JCM 4712

Sequencing of the genomes of the strain was performed on an Illumina HiSeq2500 machine. The raw data were assembled by Velvet software (v1.2.07) to obtain the scaffold. The NRPS-PKS architecture was analyzed by PKS/NRPS analysis program (<http://nrps.igs.umaryland.edu/>) online. The detailed methods and programs used for genome annotations and accurate bioinformatic analysis were according to the protocols by Xu *et al.* (Xu et al., 2018).

Fermentation and detection of MIN and related metabolites

For fermentation, *S. hygrosopicus* JCM 4712 was cultivated on MS medium (Murashige and Skoog, 1962), and a single clone was inoculated in TSB medium (Murashige and Skoog, 1962) and cultivated for 36 hr. Subsequently, the cultures (2%, V/V) were transferred to fermentation medium (Kusakabe et al., 1972), and fermented (180 r/min, 28°C) for 3 d. For HPLC and LC-HRMS analysis, the fermentation broth was processed by adding oxalic acid till pH 4.0. HPLC analysis was performed using Shimadzu LC-20AT equipped with C18 column (Shimadzu, 5 µm, 4.6 × 250 mm) under an elution gradient of 5%-20% methanol: 0.15% aqueous TFA over 30 min at a flow rate of 0.5 ml/min. LC-HRMS analysis was carried out on a Thermo Fisher Scientific ESI-LTQ Orbitrap (Scientific Inc.) controlled by Xcalibur. LC-HRMS measurements of UMP and MIN-MP (*in vivo*) were performed as previously described (Bennett et al., 2009).

Extraction and purification of MIN

The cultured broth was acidified to pH 4.0 with oxalic acid before filtration. The filtrate was collected, and extracted three times with an equal volume of ethyl acetate. The collected extract (under layer) was condensed and further dried by rotary evaporation and lyophilization. The dried residues were re-dissolved in methanol, and prepared by HPLC after passing through a 0.22 µm filter.

NMR analysis

NMR spectra of MIN were recorded on Agilent DD2 400 MHz NMR spectrometer, using D₂O as solvent.

Bioassay of MIN

For MIN bioassay, *Bacillus subtilis* CGMCC 1.338 was used as indicator strain. After incubation in Luria-Bertani medium at 37°C for 12 hr, the strain (100 µl) was mixed into melted LA medium (20 ml). Related fermentation broth (40 µl) was added into the oxford cup, and the bioassay plate was cultivated at 37°C for 12 hr to observe the antibacterial zone.

Direct cloning of the whole *min* gene cluster

The whole *min* gene cluster was directly cloned by a two-step PCR strategy, and the detailed procedure is as follows: The two pieces (Left, 5290-bp; Right, 6089-bp) housing the whole *min* gene cluster were individually amplified by KOD plus polymerase (TOYOBO) with primers (piece1-F/R and piece2-F/R) (Table S2) and template (genomic DNA of *S. hygrosopicus* JCM 4712) (Figure S1A). Treated by related enzymes, the two pieces were simultaneously cloned into the XbaI-EcoRI sites of pSET152 to give pCHW301 (Fig. S1A), which was confirmed by PCR with primers minid-F/R (Table S2).

In-frame deletion of the target *min* genes by *in vitro* CRISPR/Cas9 Editing (ICE) system

The target *min* genes were in-frame deleted by *In vitro* CRISPR/Cas9 Editing (ICE) system (Liu et al., 2015). For the construction of pCHW301 variants, the transcription templates were amplified by overlap extension PCR with primers listed in Table S2. Transcribed *in vitro* with the Transcript Aid T7 High Yield Transcription kit (Thermo; Fisher Scientific), the prepared sgRNAs (10 µg) were added into a 50 µl reaction mixture containing Cas9 protein (3 µg), pCHW301 (3 µg), and 5 µl NEBuffer 3.1 (New England Biolabs) at 37°C overnight. The reaction was terminated by addition of 2 µl RNase (0.2 mg/ml, TIANGEN Biotech) and incubated at 37°C for 15 min. Then, the reaction mixture was treated with SDS (to 1%), 1 mg/ml proteinase K, and 10 mM CaCl₂ and incubated at 55°C for 30 min. The Cas9-digested DNA was recovered by phenol-chloroform extraction and ethanol precipitation. Finally, the prepared DNA was self-ligated by T4 DNA ligase (New England Biolabs), and the ligation mixture was finally transformed into *E. coli*.

Overexpression and purification of proteins

Genes *minA* and *udk*, optimized for *E. coli* preference, were synthesized (Synbio Tech) using pET28a as the expression vector. The optimized synthetic sequences are individually shown in Table S5, S6. Expression and purification of MinA, Udk, Tdk, YeiC, MinC_N, and MinD were carried out in a similar way as described by Wu *et al.* (Wu et al., 2017). Purified proteins were concentrated and buffer-exchanged into protein stock buffer (25 mM Tris, 150 mM NaCl, and 10% glycerol, pH 7.0 for MinA, Udk, and Tdk, pH 7.5 for YeiC, MinC_N, and MinD) using Amicon Ultra filters. The final proteins were flash-frozen in liquid nitrogen and stored at -80°C.

***In vitro* assay of MinA**

For activity assay of MinA, reaction, consisting of 50 mM Tris buffer (pH 7.0), 1 mM L-Gln, 1 mM FMN, 5 mM MgCl₂, 2 mM ATP and 20 µg MinA, was performed at 18°C (or other related temperature) overnight. Reaction was then terminated by addition of equivalent volume of methanol. Following centrifugation to remove the

supernatant, 100 μ l DMSO was added to dissolve the sediment. The reaction was analyzed by HPLC and LC-HRMS equipped with a reverse phase C18 column with 0.15% aqueous TFA (70%): methanol (30%) to 0.15% aqueous TFA (50%): methanol (50%) at a flow rate of 0.5 ml/min over 20 min.

***In vitro* assay of Udk, Tdk, YeiC, and MinC_N**

For Udk (from *Bacillus subtilis*), Tdk and YeiC (from *S. coelicolor*) activity assay, reactions consisting of 50 mM Hepes buffer (pH 7.0), 1 mM MIN, 10 mM MgCl₂, 1 mM ATP, and 20 μ g protein was performed at 30°C. The reaction mixtures were added to ultrafiltration tube to remove protein by centrifugation after 4 hr, and the remaining reaction mixture was then collected. For MinC_N activity assay, the FastAP buffer (Thermo Scientific) and 20 μ g MinC_N were added to the collected reaction mixture and incubated at 30°C. Reaction was terminated by the addition of methanol (equivalent volume) after 1 hr. Following centrifugation to remove protein, the reactions were analyzed by LC-HRMS equipped with a reverse phase C18 column.

***In vitro* assay of MinD**

For activity assay of MinD, reaction consisting of 50 mM Tris buffer (pH 7.5), 1 mM 5-phosphoribose-1-pyrophosphate (PRPP), 10 mM MgCl₂, 1 mM uracil, and 20 μ g MinD, was conducted at 30°C. Reaction was terminated by the addition of equivalent volume of methanol after 4 hr. Following centrifugation to remove protein, the reactions were analyzed by HPLC equipped with a reverse phase C18 column with detection at 254 nm and a flow rate of 0.5 ml/min. The HPLC condition is as follows: solvent system A (0.15% aqueous TFA) and B (methanol) run over a linear gradient of 90%-70% in 15 min.

The cloning and *in vivo* functional analysis of *minD*, *minT*, *minC_N*

The recombinant plasmids (pIB139/*minD*, pIB139/*minT*, pIB139/*minC_N*, pIB139/*minDT*, pIB139/*minDC_N*, pIB139/*minTC_N*, pIB139/*minDTC_N*) were constructed according to the standard protocols of Green *et al.* (Green and Sambrook, 2002) or

Kieser *et al.* (Kieser et al., 2000). Taking pIB139/*minDTC_N* as example, *minD* was cloned into pIB139 and the positive plasmid was named pIB139/*minD*. The *minT* was cloned into pJTU968 and digested to obtain the (*PerME*+minT*) fragment. The digested fragment was ligated to pIB139/*minD* in EcoRI site with correct orientation, and the resulting positive plasmid was named pIB139/*minDT*. Likewise, pIB139/*minDTC_N* was constructed and designated. After construction, all of the target plasmids were individually introduced into *S. coelicolor* M1154. For plate-grown experiments (30°C), corresponding recombinant strains were inoculated to the related rectangular area of a plate containing MIN (10 µg/ml).

4. References

- Bennett, B.D., Kimball, E.H., Gao, M., Osterhout, R., Van Dien, S.J., and Rabinowitz, J.D. (2009). Absolute metabolite concentrations and implied enzyme active site occupancy in *Escherichia coli*. *Nat Chem Biol* 5, 593-599.
- Bierman, M., Logan, R., O'Brien, K., Seno, E.T., Rao, R.N., and Schoner, B.E. (1992). Plasmid cloning vectors for the conjugal transfer of DNA from *Escherichia coli* to *Streptomyces* spp. *Gene* 116, 43-49.
- Gomez-Escribano, J.P., and Bibb, M.J. (2014). Heterologous expression of natural product biosynthetic gene clusters in *Streptomyces coelicolor*: from genome mining to manipulation of biosynthetic pathways. *J Ind Microbiol Biotechnol* 41, 425-431.
- Green, M.R., and Sambrook, J. (2002). *Molecular Cloning: a Laboratory Manual*, 3rd ed., Cold Spring Harbor Laboratory Press, NY.
- Kieser, T., Bibb, M.J., Chater, K.F., Butter, M.J., and Hopwood, D.A. (2000). *Practical Streptomyces Genetics*, 2nd ed., John Innes Foundation, Norwich, United Kingdom.
- Kusakabe, Y., Nagatsu, J., Shibuya, M., Kawaguchi, O., and Hirose, C. (1972). Minimycin, a new antibiotic. *J Antibiot (Tokyo)* 25, 44-47.
- Liu, Y., Tao, W., Wen, S., Li, Z., Yang, A., Deng, Z., and Sun, Y. (2015). *In Vitro* CRISPR/Cas9 System for efficient targeted DNA editing. *Mbio* 6, e01714-01715.
- Murashige, T., and Skoog, F. (1962). A revised medium for rapid growth and bio assays with tobacco tissue cultures. *Physiol Plantarum* 15, 473-497.
- Vecchio, F.D., Petkovic, H., Kendrew, S.G., Low, L., Wilkinson, B., Lill, R., Cortés, J., Rudd, B.A.M., Staunton, J., and Leadlay, P.F. (2003). Active-site residue, domain and module swaps in modular polyketide synthases. *J Ind Microbiol Biotechnol* 30, 489-494.
- Wu, P., Wan, D., Xu, G., Wang, G., Ma, H., Wang, T., Gao, Y., Qi, J., Chen, X., Zhu, J., *et al.* (2017). An unusual protector-protege strategy for the biosynthesis of purine nucleoside antibiotics. *Cell*

Chem Biol 24, 171-181.

Xu, G., Kong, L., Gong, R., Xu, L., Gao, Y., Jiang, M., Cai, Y.-S., Hong, K., Hu, Y., Liu, P., *et al.* (2018). Coordinated biosynthesis of the purine nucleoside antibiotics aristeromycin and coformycin in *Actinomycetes*. *Appl Environ Microbiol* 84, e01860-01818.

Zhou, X., Wu, H., Li, Z., Zhou, X., Bai, L., and Deng, Z. (2011). Over-expression of UDP-glucose pyrophosphorylase increases validamycin A but decreases validoxylamine A production in *Streptomyces hygrosopicus* var. *jinggangensis* 5008. *Metab Eng* 13, 768-776.